

# Supporting Information

## Programmed Negative Allostery with Guest-selected Rotamers Control Anion-anion Complexes of Stackable Macrocycles

Edward G. Sheetz, Bo Qiao, Maren Pink, and Amar H. Flood\*

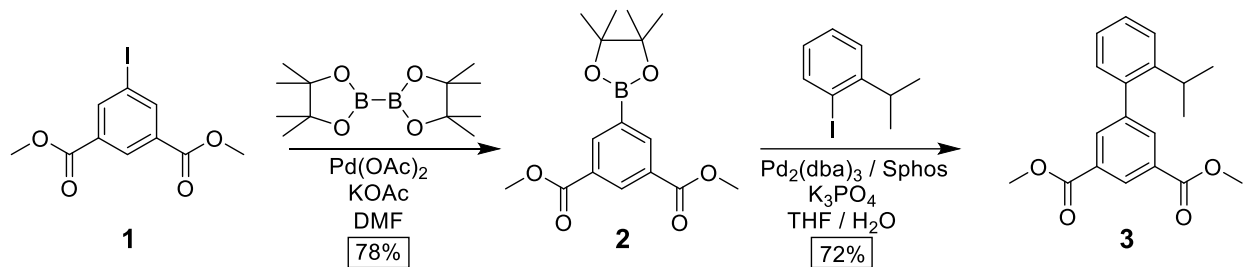
- S1. General Methods
- S2. Synthesis and Compound Characterization
- S3. Variable Concentration Spectra of Cyanodimer
- S4.  $^1\text{H}$ -NMR Titrations of Cyanostar and Cyanodimer with Bisulfate in  $\text{CDCl}_3$
- S5.  $^1\text{H}$ -NMR Titrations of Cyanostar and Cyanodimer with Bisulfate in  $\text{CD}_2\text{Cl}_2$
- S6. 2D-ROESY NMR Spectrum of Cyanodimer:bisulfate Complex
- S7. ESI Mass Spectra of a Cyanodimer:bisulfate Mixture
- S8. Torsional Entropy Calculations
- S9. Conformational Entropy Calculations
- S10.  $^1\text{H}$ -NMR Titrations of Cyanostar and Cyanodimer with Perchlorate in  $\text{CD}_2\text{Cl}_2$
- S11. Variable Temperature  $^1\text{H}$ -NMR Titrations of Cyanostar and Cyanodimer with Perchlorate in  $\text{C}_2\text{D}_2\text{Cl}_4$
- S12. Variable Temperature UV-Visible Titrations of Cyanostar and Cyanodimer with Perchlorate in  $\text{C}_2\text{H}_4\text{Cl}_2$
- S13. Configurational Information for the Preliminary Crystal Structure
- S14.  $^1\text{H}$  and  $^{13}\text{C}$  NMR Spectra

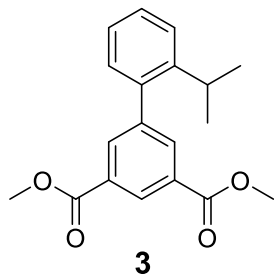
## S1. General Methods

Reagents were obtained from commercial suppliers and used as received unless otherwise noted. Dimethyl 5-iodoisophthalate (**1**)<sup>S1</sup> and dimethyl 5-(4,4,5,5-tetramethyl-1,3,2-dioxaborolan-2-yl)isophthalate (**2**)<sup>S1</sup> were prepared according to reported procedures. Column chromatography was performed on silica gel (160–200 mesh) or alumina neutral (32–63  $\mu\text{m}$ , #060223L, Sorbent Technologies, USA). Thin-layer chromatography (TLC) was performed on pre-coated silica gel plates (0.25 mm thick, #1615126, Sorbent Technologies, USA) and observed under UV light. Nuclear magnetic resonance (NMR) spectra were recorded on Varian Inova (400 MHz), Varian Inova (500 MHz), Varian Inova (600 MHz) and Varian VXR (400 MHz) spectrometers at room temperature (298 K). Chemical shifts were referenced on tetramethylsilane (TMS) or residual solvent peaks. High resolution electrospray ionization (ESI) mass spectrometry was performed on a Thermo Electron Corporation MAT 95XP-Trap mass spectrometer. Our current data set for the cyanodimer:perchlorate crystal structure lacks high resolution data (beyond 1.5 Å), which could not be mitigated, even with excessive exposure times. This is a known pathology for highly disordered cyanostar structures<sup>S2-S11</sup> with large, solvent accessible areas. The unit cell, space group and packing are unambiguously established. However, the structure cannot be fully determined and refined because of a lack of data.

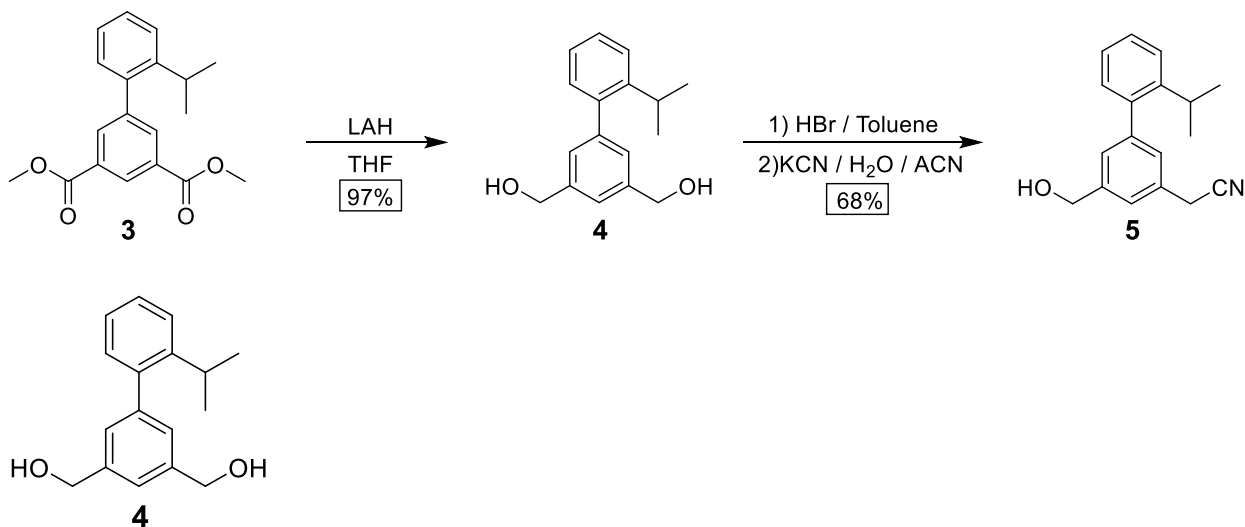
## S2. Synthesis and Compound Characterization

Cyanodimer was prepared (Scheme 1) using a modification of the synthesis of the cyanosolo macrocycle. With Suzuki coupling undertaken (step 2) prior to ester reduction (step 3), side reactions involving palladium complexes and benzyl alcohols in water are avoided while also allowing for facile reduction of the ester. Macrocyclization proceeded in a one-pot Knoevenagel cyclocondensation from aldehyde monomer in a 38% yield.



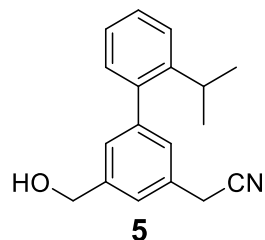


**Dimethyl 2'-isopropyl-[1,1'-biphenyl]-3,5-dicarboxylate (3):** **2** (2.10 g, 6.56 mmol), potassium phosphate tribasic (4.18 g, 19.68 mmol), tris(dibenzylideneacetone)dipalladium(0) (0.300 g, 0.328 mmol), and 2-dicyclohexylphosphino-2',6'-dimethoxybiphenyl (0.269 g, 0.656 mmol) were combined in a round-bottom flask and degassed with argon. 1-Iodo-2-isopropylbenzene (2.02 g, 7.87 mmol) dissolved in distilled tetrahydrofuran (50 mL) were added via syringe, followed by argon-degassed H<sub>2</sub>O (50 mL). The solution was then stirred at 60 °C for 16 hours. The product was then extracted with EtOAc (3 × 50 mL), and the organic layer was dried with magnesium sulfate and concentrated in vacuo. The crude product was purified by silica gel column chromatography (6% EtOAc in hexanes), yielding **3** (1.43 g, 4.58 mmol, 70% yield) as a white, crystalline solid. <sup>1</sup>H-NMR (500 MHz, CD<sub>2</sub>Cl<sub>2</sub>) δ (ppm) = 8.60 (t, *J* = 1.6 Hz, 1H), 8.13 (d, *J* = 1.6 Hz, 2H), 7.40 (dd, *J* = 1.5, 7.9 Hz, 1H), 7.36 (dt, *J* = 1.4, 8.0 Hz, 1H), 7.21 (dt, *J* = 1.6, 7.6 Hz, 1H), 7.13 (dd, *J* = 1.3, 7.6 Hz, 1H), 3.90 (s, 6H), 2.89 (sep, *J* = 6.8 Hz, 1H), 1.12 (d, *J* = 6.8 Hz, 6H). <sup>13</sup>C NMR (125 MHz, CD<sub>2</sub>Cl<sub>2</sub>) δ (ppm) = 166.1, 146.3, 142.8, 139.0, 134.4, 130.6, 129.7, 128.8, 128.4, 125.7, 125.5, 52.2, 29.5, 23.8. HR-ESI-MS: C<sub>19</sub>H<sub>20</sub>O<sub>4</sub> M<sup>+</sup>, Calculated: 312.1362, Found: 312.1358

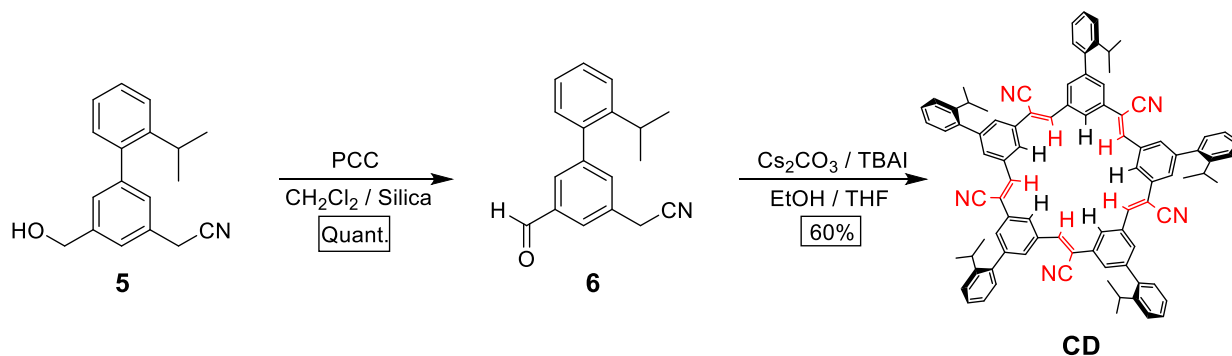


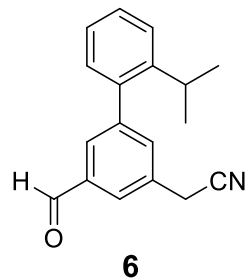
**2'-Isopropyl-[1,1'-biphenyl]-3,5-diyl dimethanol (4):** Lithium aluminum hydride (0.281 g, 7.49 mmol) was suspended in tetrahydrofuran (50 mL), and **3** (1.05 g, 3.36 mmol) was added dropwise dissolved in tetrahydrofuran. The solution was heated at reflux for 4 hours. The reaction was quenched by addition of H<sub>2</sub>O (0.3 mL), then conc. aq. NaOH (0.3 mL), followed by H<sub>2</sub>O (1 mL). The solution was then filtered, and the cake was washed with EtOAc. The filtrate was then washed with brine, dried with magnesium sulfate, and concentrated in vacuo, yielding **4** (8.197 g, 3.25 mmol, 97% yield). <sup>1</sup>H-NMR (500 MHz, CD<sub>2</sub>Cl<sub>2</sub>) δ (ppm) = 7.37 (dd, *J* = 1.2, 7.8 Hz, 1H), 7.35 (s,

1H), 7.31 (dt,  $J = 1.3, 7.3$  Hz, 1H), 7.18 (m, 3H), 7.12 (dd,  $J = 1.5, 7.6$  Hz, 1H), 4.71 (d,  $J = 5.9$  Hz, 4H), 3.00 (sep,  $J = 6.9$  Hz, 1H), 1.77 (t,  $J = 5.9$  Hz, 2H), 1.13 (d,  $J = 6.9$  Hz, 6H).  $^{13}\text{C}$  NMR (125 MHz,  $\text{CD}_2\text{Cl}_2$ )  $\delta$  (ppm) = 146.0, 142.3, 141.3, 141.0, 129.4, 127.3, 126.4, 125.1, 124.9, 123.6, 63.7, 29.1, 23.2. HR-ESI-MS:  $\text{C}_{17}\text{H}_{20}\text{O}_2 \text{M}^+$  Calculated: 254.1643, Found: 254.1639.

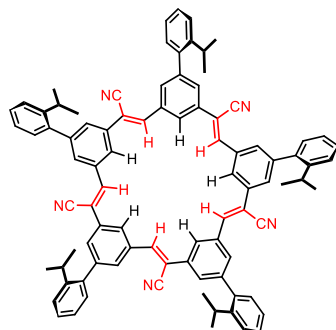


**2-(5-(Hydroxymethyl)-2'-isopropyl-[1,1'-biphenyl]-3-yl)acetonitrile (5):** Diol **4** (0.820 g, 3.25 mmol) was dissolved in toluene at  $70^\circ\text{C}$ , and 0.55 48% aq. HBr was added dropwise to the stirring solution. The reaction was allowed to stir for 12 hours at  $70^\circ\text{C}$ , then it was cooled to room temperature. The toluene was concentrated in vacuo, and the crude product was redissolved  $\text{CH}_2\text{Cl}_2$ . The organic phase was washed with sodium carbonate and brine, dried with magnesium sulfate, and concentrated in vacuo. The crude product was then dissolved in acetonitrile at  $60^\circ\text{C}$ , and KCN dissolved in  $\text{H}_2\text{O}$  was added dropwise to the stirring solution. The solution was allowed to stir at  $60^\circ\text{C}$  for 16 hours, then the solution was cooled to room temperature. The acetonitrile was removed by rotary evaporation, and the product was extracted with EtOAc ( $3 \times 50$  mL). The organic phase was washed with sodium carbonate and brine, dried with magnesium sulfate, and concentrated in vacuo. The crude product was purified by silica gel column chromatography (20% EtOAc in hexanes), yielding **5** (0.592 g, 2.36 mmol, 69% yield).  $^1\text{H}$ -NMR (500 MHz,  $\text{CD}_2\text{Cl}_2$ )  $\delta$  (ppm) = 7.38 (dd,  $J = 1.65, 9.7$  Hz, 1H), 7.33 (m, 3H), 7.22 (s, 1H), 7.19 (dt,  $J = 1.8, 9.5$  Hz, 1H), 7.15 (s, 1H), 7.11 (dd,  $J = 1.3, 9.5$  Hz, 1H), 4.72 (d,  $J = 7.25$  Hz, 2H), 3.80 (s, 2H), 2.97 (sep,  $J = 8.5$  Hz, 1H), 1.90 (t,  $J = 7.35$  Hz, 1H), 1.14 (d,  $J = 8.5$  Hz, 6H).  $^{13}\text{C}$  NMR (125 MHz,  $\text{CDCl}_3$ )  $\delta$  (ppm) = 146.27, 143.35, 141.96, 139.97, 129.93, 129.78, 128.11, 127.96, 127.44, 125.69, 125.44, 124.75, 117.96, 64.56, 29.49, 24.30, 23.57. HR-ESI-MS:  $\text{C}_{18}\text{H}_{19}\text{NO} \text{M}^+$  Calculated: 265.1467, Found: 265.1461.





**2-(5-Formyl-2'-isopropyl-[1,1'-biphenyl]-3-yl)acetonitrile (6):** Alcohol **5** (0.300 g, 1.19 mmol) was dissolved in dichloromethane, to which a mixture of pyridinium chlorochromate (0.310 g, 1.40 mmol) and silica gel (0.450 g) was added. The mixture was allowed to stir at room temperature for 12 hours, at which time it was poured directly onto a column of silica gel and purified by silica gel column chromatography (dichloromethane), yielding **6** (0.296 g, 1.19 mmol, quant. yield). <sup>1</sup>H-NMR (400 MHz, CD<sub>2</sub>Cl<sub>2</sub>) δ (ppm) = 10.05 (s, 1H), 7.86 (s, 1H), 7.77 (s, 1H), 7.57 (s, 1H), 7.43 (dd, *J* = 0.9, 7.8 Hz, 1H), 7.39 (dt, *J* = 1.2, 7.9 Hz, 1H), 7.24 (dt, *J* = 1.2, 7.4 Hz, 1H), 7.16 (dd, *J* = 1.1, 7.6 Hz, 1H), 3.91 (s, 2H), 2.96 (sep, *J* = 6.8 Hz, 1H), 1.17 (d, *J* = 6.8 Hz, 6H). <sup>13</sup>C NMR (100 MHz, CD<sub>2</sub>Cl<sub>2</sub>) δ (ppm) = 191.4, 146.3, 144.0, 138.8, 136.9, 134.5, 131.4, 130.3, 129.6, 128.5, 126.9, 125.8, 125.5, 117.3, 29.5, 23.9, 23.4. HR-ESI-MS: C<sub>18</sub>H<sub>17</sub>NO M<sup>+</sup> Calculated: 263.1310, Found: 263.1304.



**2-Isopropylphenylcyanostar (cyanodimer):** Cesium carbonate was dissolved in absolute ethanol (85 mL) at 50 °C. Tetrahydrofuran (85 mL) was added and the solution was allowed to cool to room temperature. Aldehyde **6** (0.2105 g, 0.84 mmol) was dissolved in tetrahydrofuran (5 mL) and added to the stirring solution. The reaction vessel was covered in aluminum foil to protect it from light. The solution was allowed to stir for 48 hours at room temperature, then it was concentrated in vacuo, redissolved in dichloromethane, and filtered to remove solid cesium carbonate. The filtrate was then dried with magnesium sulfate and concentrated in vacuo. The crude product was purified by silica gel column chromatography (chloroform) yielding cyanodimer (0.0788 g, 0.06 mmol, 38% yield) as a yellow powder. <sup>1</sup>H-NMR (400 MHz, CD<sub>2</sub>Cl<sub>2</sub>) δ (ppm) = 8.53 (s, 5H), 7.96 (s, 5H), 7.95 (s, 5H), 7.81 (s, 5H), 7.42 (m, 10H), 7.27 (m, 10H), 3.11 (sep, *J* = 6.8 Hz, 5H), 1.23 (d, *J* = 6.8 Hz, 30H). HR-ESI-MS: C<sub>90</sub>H<sub>75</sub>N<sub>5</sub> [M + I]<sup>-</sup>, Calculated: 1352.5073, Found: 1352.5123

### S3. Variable Concentration Spectra of Cyanodimer

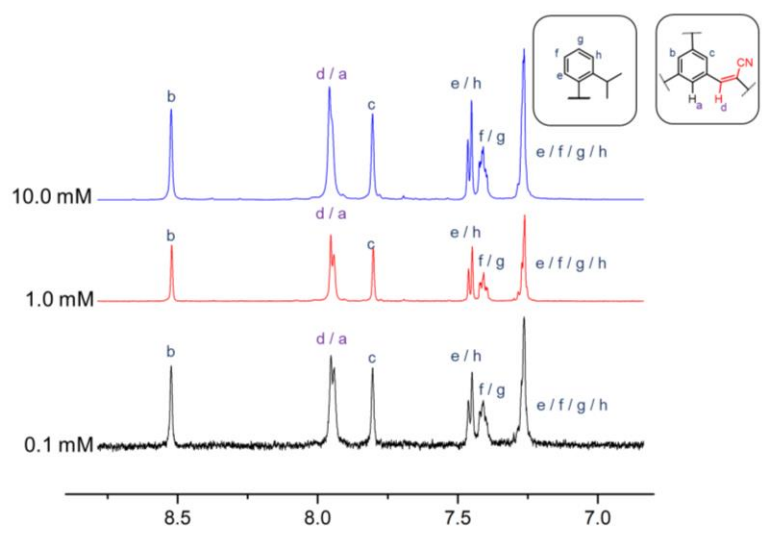


**Figure S1.**  $^1\text{H}$  NMR Spectra of cyanodimer at various concentrations ( $\text{CD}_2\text{Cl}_2$ , 298 K, 600 MHz)

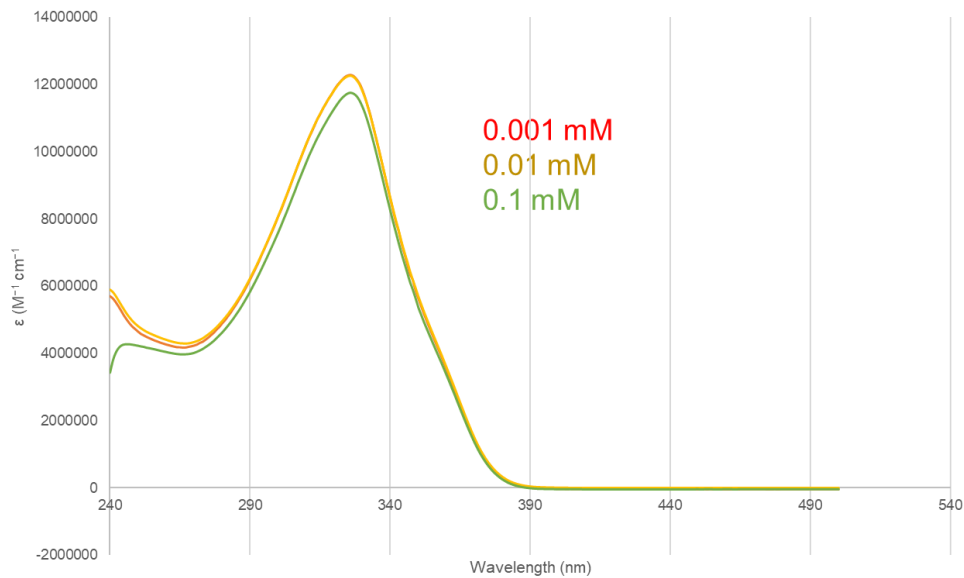


**Figure S2.** UV-Vis absorption spectra of cyanodimer at 0.1, 0.01, and 0.001 mM in  $\text{CH}_2\text{Cl}_2$  (absorbance was divided by concentration and path length to give extinction coefficient).

#### S4. $^1\text{H-NMR}$ Titrations of Cyanostar and Cyanodimer with Bisulfate in $\text{CDCl}_3$

Eq.  $\text{HSO}_4^-$

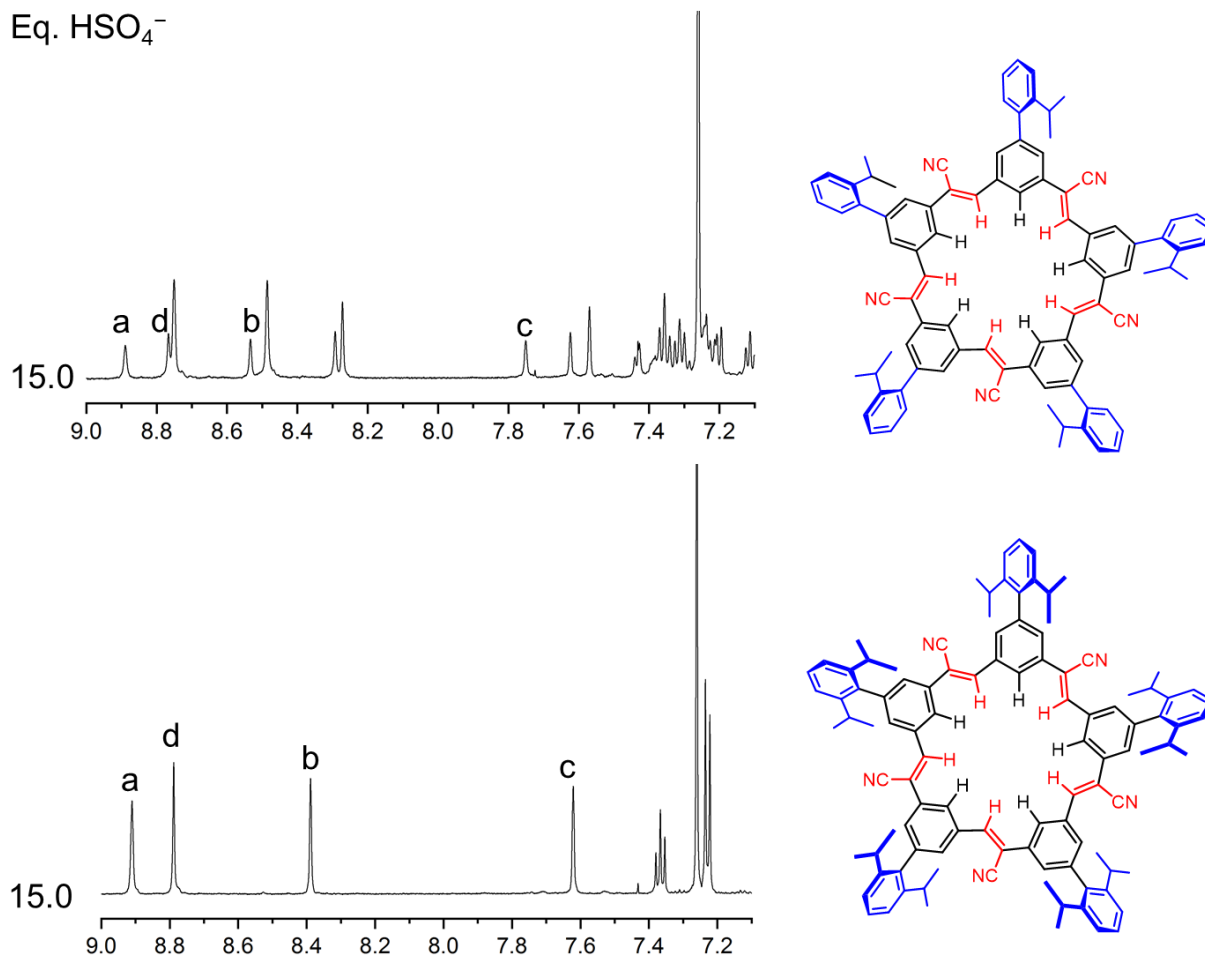


**Figure S3.**  $^1\text{H-NMR}$  spectra for cyanosolo (1 mM,  $\text{CDCl}_3$ , 298 K, 600 MHz) and cyanodimer (1 mM,  $\text{CDCl}_3$ , 298 K, 600 MHz) 15 eq of  $\text{HSO}_4^-$ . The analogous peak positions between the inner proton peaks for cyanosolo and the new species in cyanodimer supports the assignment as a 1:1 complex. Peak labels are identical to other titrations and identifications for cyanodimer are based on analogy to cyanosolo.

## S5. $^1\text{H}$ -NMR Titrations of Cyanostar and Cyanodimer with Bisulfate in $\text{CD}_2\text{Cl}_2$

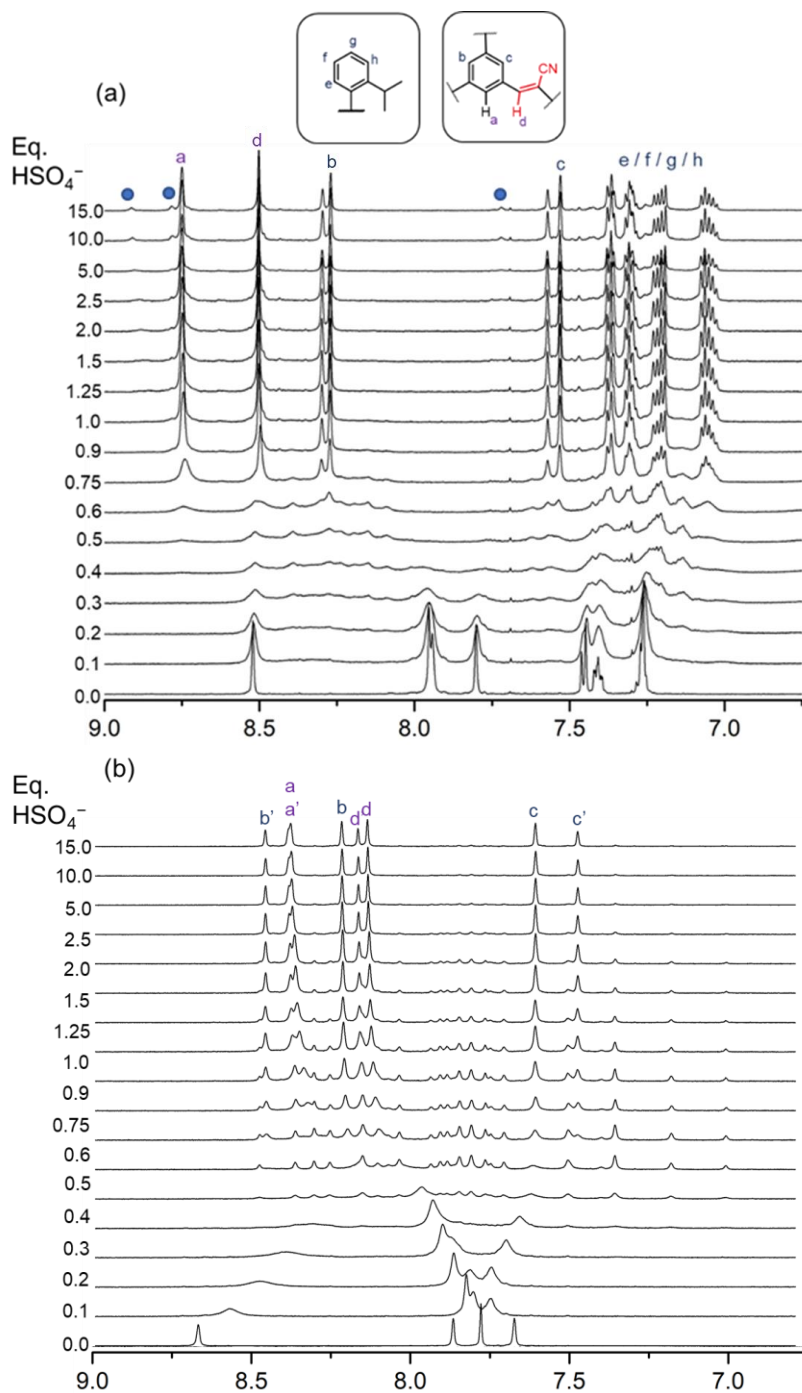


**Figure S4.** Aromatic regions of  $^1\text{H}$  NMR titration data. (a)  $\text{HSO}_4^-$  titration with cyanodimer (1 mM,  $\text{CD}_2\text{Cl}_2$ , 298 K, 600 MHz). The 1:1 complex is labelled with blue dots. (b)  $\text{HSO}_4^-$  titration with cyanostar (1 mM,  $\text{CD}_2\text{Cl}_2$ , 298 K, 600 MHz). Peak labels are for the 2:2 complex; there are no resonances above 10 ppm.

## S6. 2D ROESY Spectrum of Cyanodimer:bisulfate 2:2 Complex

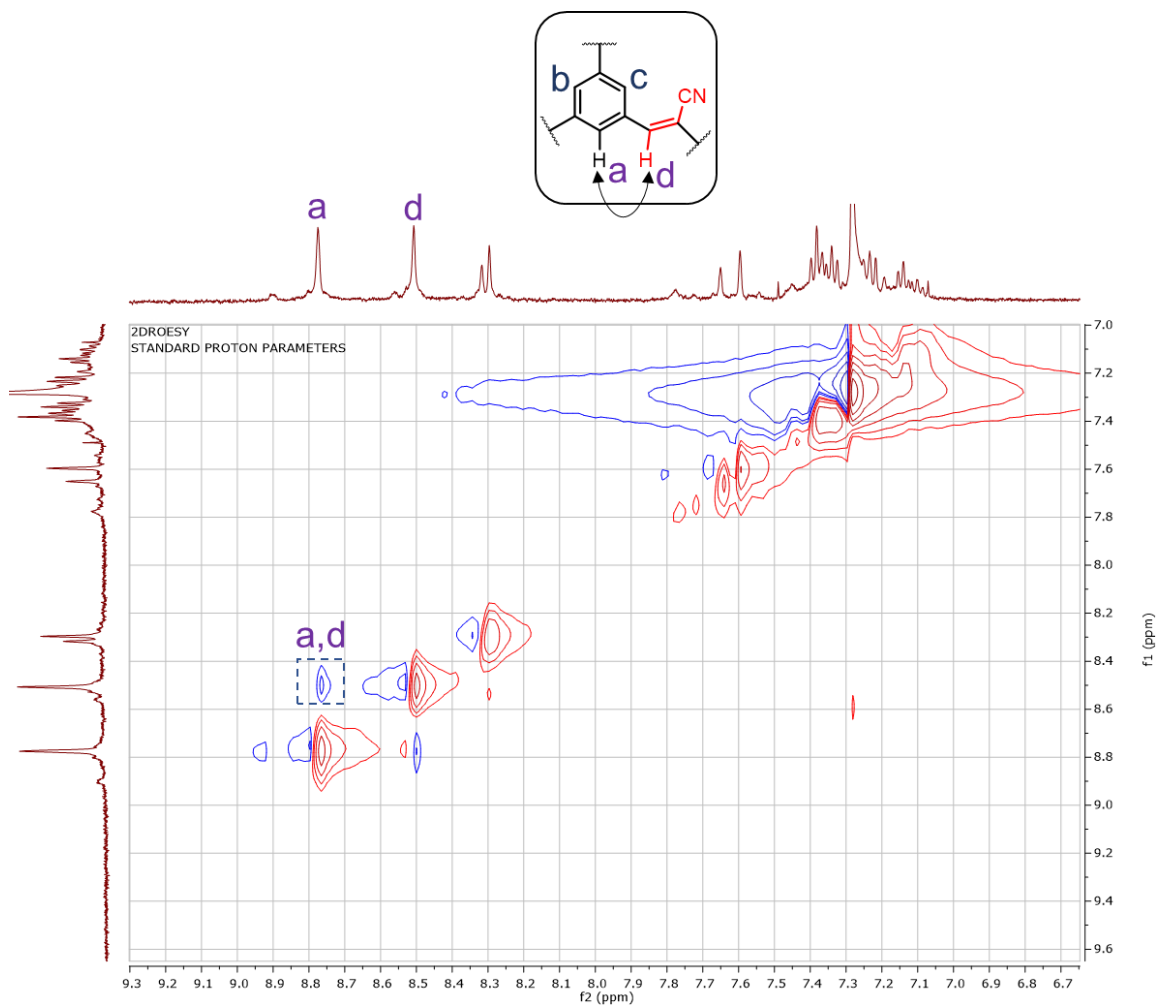


**Figure S5.** 2D ROESY spectrum of a 2:2 cyanodimer bisulfate complex demonstrating through-space correlation between protons H<sup>a</sup> and H<sup>d</sup> (1 mM, 298 K, CDCl<sub>3</sub>, 500 MHz).

## S7. ESI Mass Spectra of a Cyanodimer:bisulfate Mixture

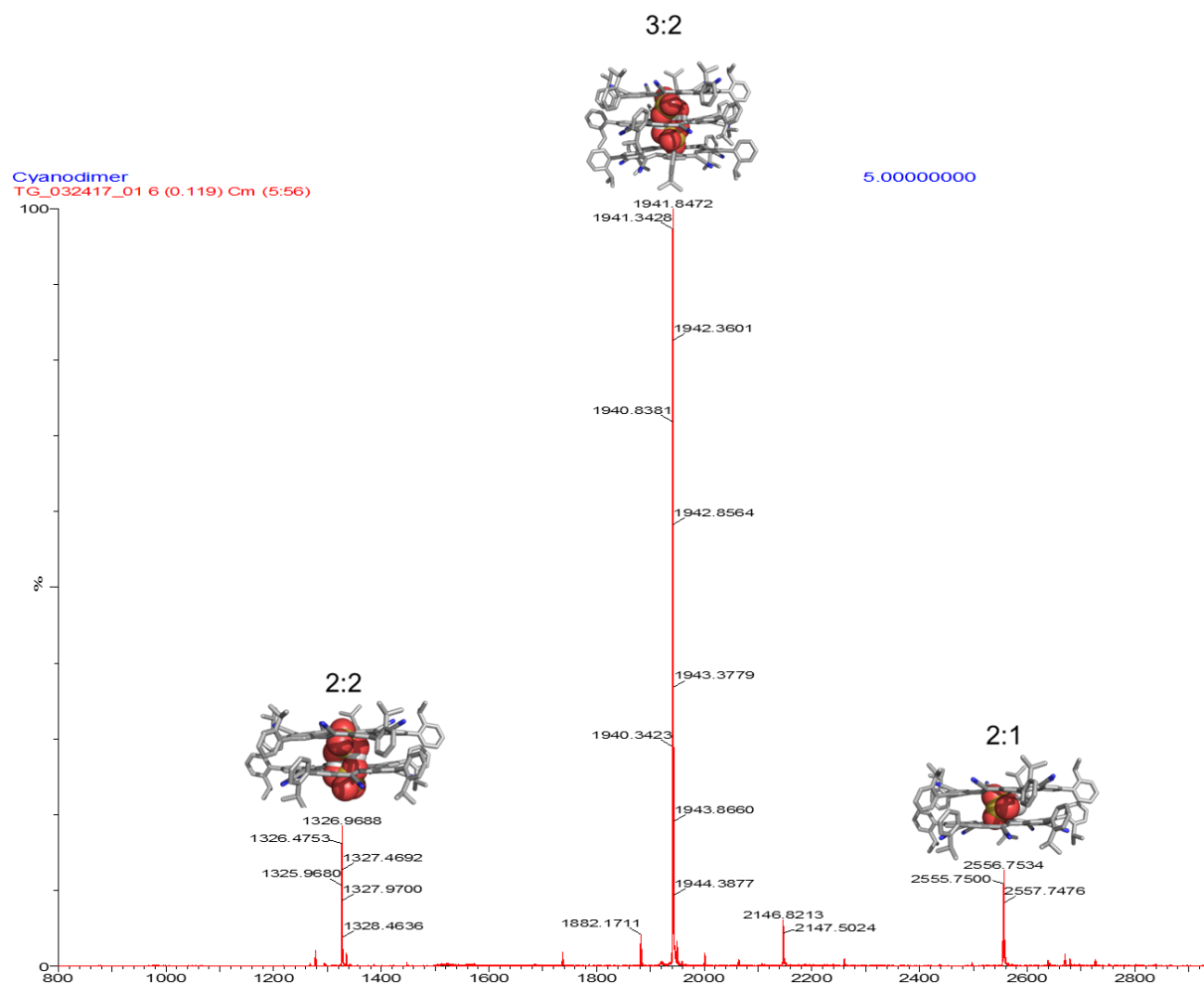


**Figure S6a.** ESI Mass spectrum of a 2:1 mixture of cyanodimer and tetrabutylammonium bisulfate (2 mM, CH<sub>2</sub>Cl<sub>2</sub>, 50 °C source, 20 V cone voltage).

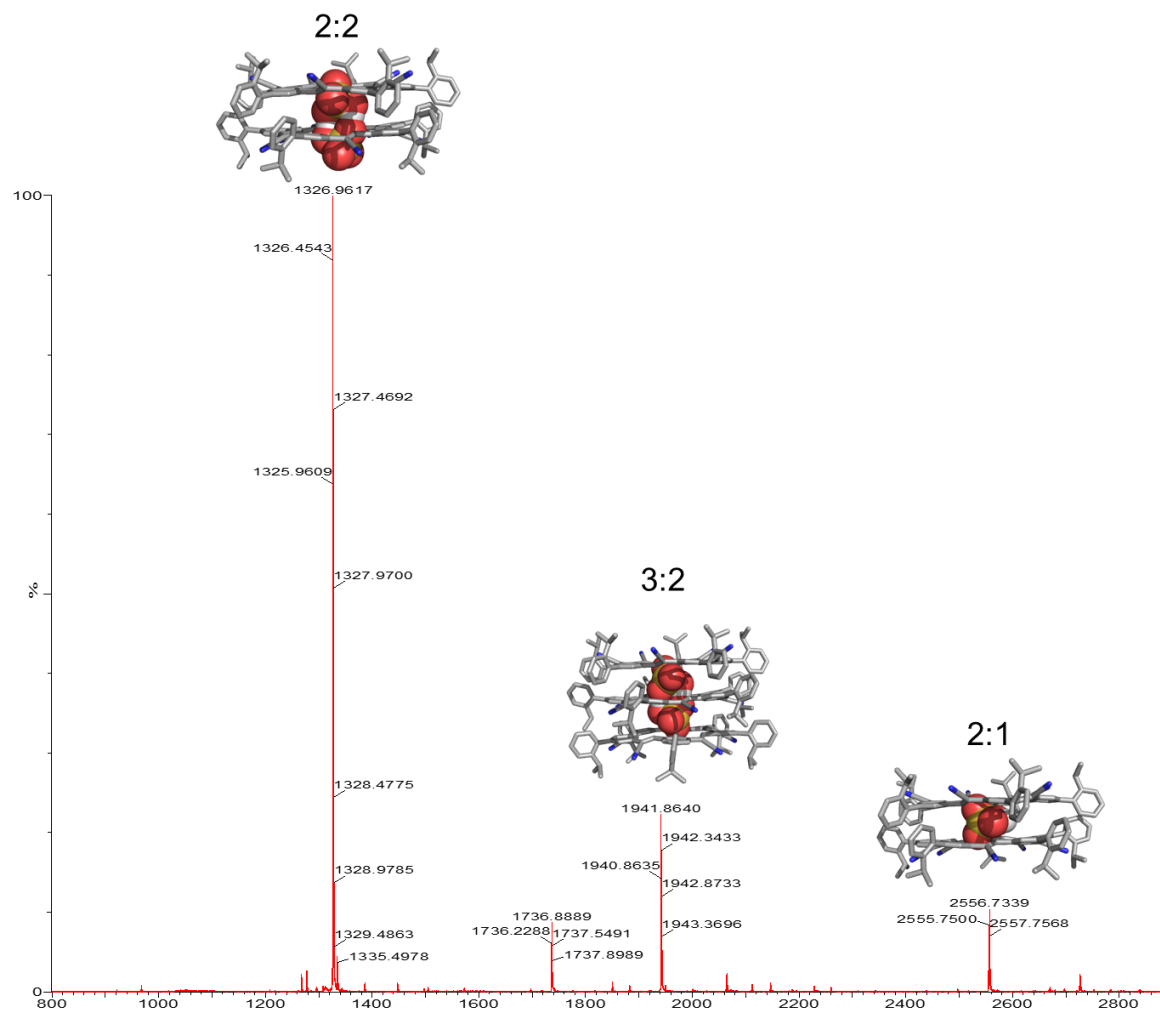


**Figure S6b.** ESI Mass spectrum of a 1:1 mixture of cyanodimer and tetrabutylammonium bisulfate (2 mM, CH<sub>2</sub>Cl<sub>2</sub>, 50 °C source, 20 V cone voltage). This demonstrates a significant suppression of the 3:2 complex relative to other complexes when compared to the parent cyanostar under the same conditions.<sup>S5</sup>

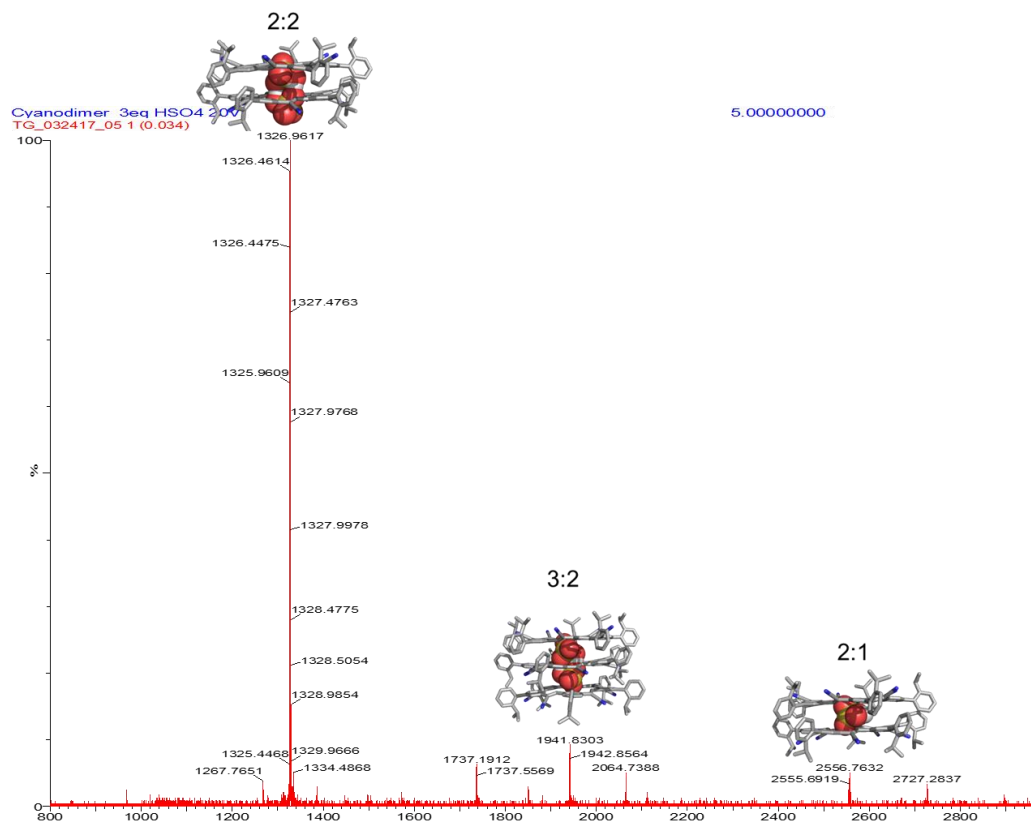


**Figure S6c.** ESI Mass spectrum of a 1:4 mixture of cyanodimer and tetrabutylammonium bisulfate (2 mM,  $\text{CH}_2\text{Cl}_2$ , 50 °C source, 20 V cone voltage). This demonstrates a significant suppression of the 3:2 complex relative to other complexes when compared to the parent cyanostar under the same conditions.<sup>S5</sup>

### **S8. Model of a Cyanodimer:bisulfate 3:2 Complex**

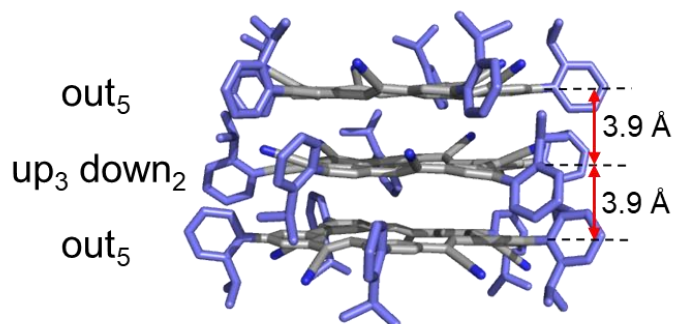


**Figure S7.** Molecular model of a cyanodimer:bisulfate 3:2 complex (bisulfate omitted) energy-minimized using molecular mechanics. The interplanar distance between each pair of macrocycles is listed.

## S8. Torsional Entropy Calculations

Torsional entropy calculations were used to estimate the entropy change associated with the dimerization of cyanostars arising from change in rotational characteristics of the biphenyl substituents. The calculations were performed using the following equations from Whitesides and coworkers:<sup>S12</sup>

$$S_{\text{tor}} = \int_{\Phi=0}^{2\pi} P \ln P \, d\Phi \quad \text{Eq S1}$$

$$P = \frac{e^{-E/kT}}{\int_{\Phi=0}^{2\pi} e^{-E/kT} \, d\Phi} \quad \text{Eq S2}$$

Here,  $S_{\text{tor}}$  is the change in torsional entropy when a bond is allowed to rotate freely,  $P$  is the probability of the molecule existing in a rotational conformation of a given energy,  $E$ , which is defined for each angle  $\Phi$  around a single bond.  $T$  is defined as being 300 K.

For this calculation, a model compound was used that represents one of cyanodimer's biphenyl units (Figure S8). We use this model under the assumption that each biphenyl bond rotates independently from each other. Relative energies were calculated using density functional theory (B3LYP/6-31G\*) as a function of angle at 22.5° increments. Under the assumption that the rotation around each biphenyl bond becomes restricted upon macrocycle dimerization, these rotational energy profiles were used with the above equations (Eq 1 and Eq 2) to calculate a loss in torsional entropy of 12.3 J mol<sup>-1</sup> K<sup>-1</sup> for each biphenyl unit. A total of 123 J mol<sup>-1</sup> K<sup>-1</sup> is associated with restricting the rotation of 10 biphenyl units in a dimer of macrocycles corresponding to a loss of ~34 kJ mol<sup>-1</sup> in free energy at 300 K.

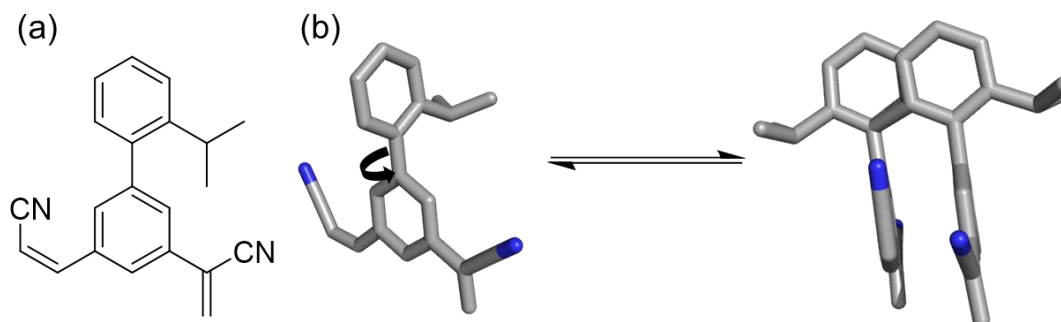


**Figure S8.** (a) Monomer used for torsional energy calculations, and (b) the rotational freedom of the biphenyl bond as a monomer and a dimer.

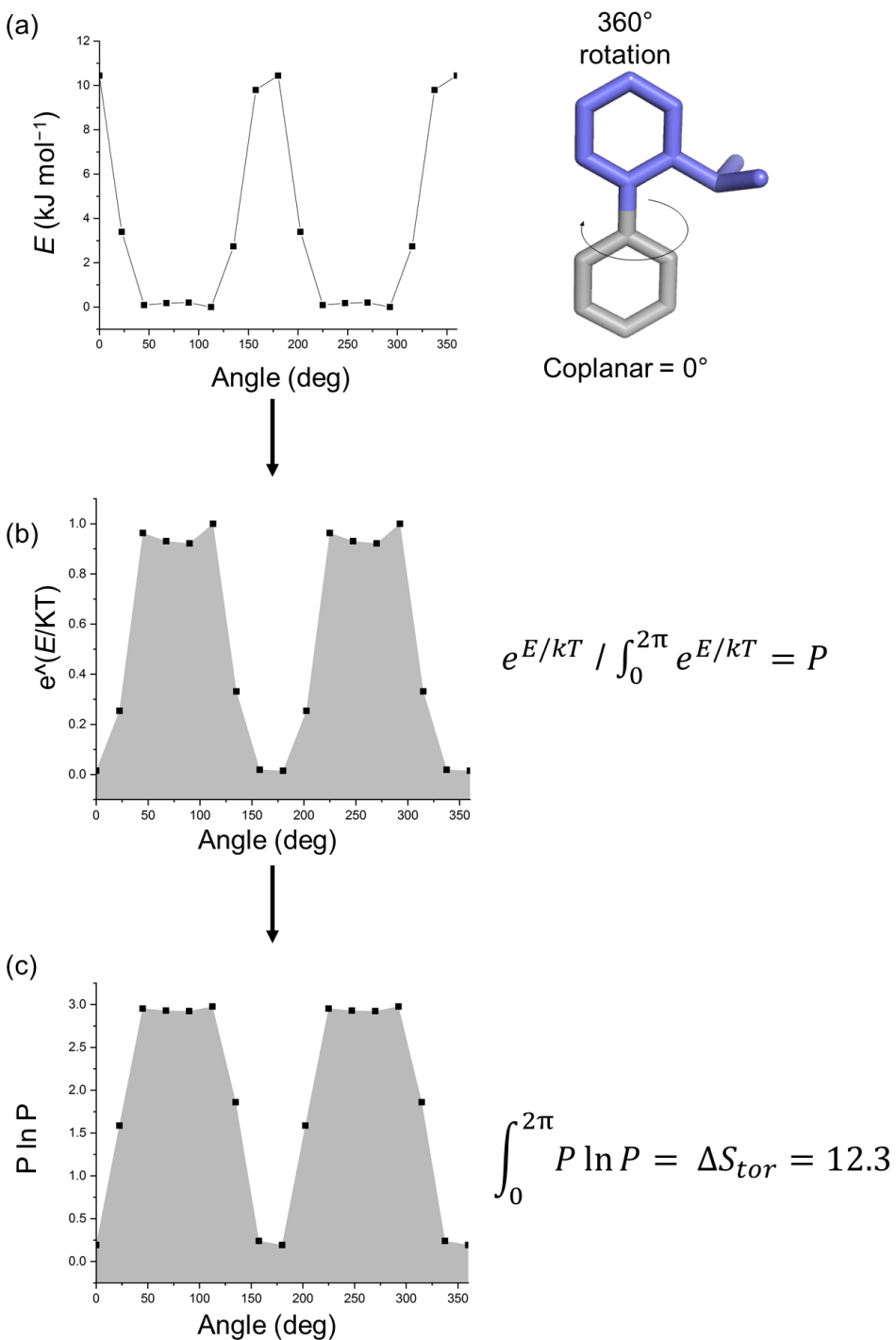


**Figure S9** (a) The calculated potential energy map for the rotation of the biphenyl bond in the model compound (B3LYP/6-31g\*). (b) The probability,  $P$ , of each energy state being populated is calculated according to Eq. 2 by dividing  $\exp(E/kT)$  by its integral from 0 to  $2\pi$  for each energy  $E$ . (c) The change in torsional entropy is calculated by integrating  $P \ln P$  from 0 to  $2\pi$ .

## S9. Conformational Entropy Calculations

Conformational entropy calculations were used to estimate the lower bound of the entropy change associated with dimerization of cyanodimer in the 2:1 complexes. In the free cyanodimer, there are six distinct rotational isomers with differing numbers of degeneracies (Figure S10a) based on whether the exterior isopropyl groups are facing upwards or downwards. If we assume that all of these conformations are equally populated (within thermal energy  $RT = 0.6 \text{ kcal mol}^{-1}$ ), then one cyanodimer has 32 degenerate conformations it can adopt (Figure S10).

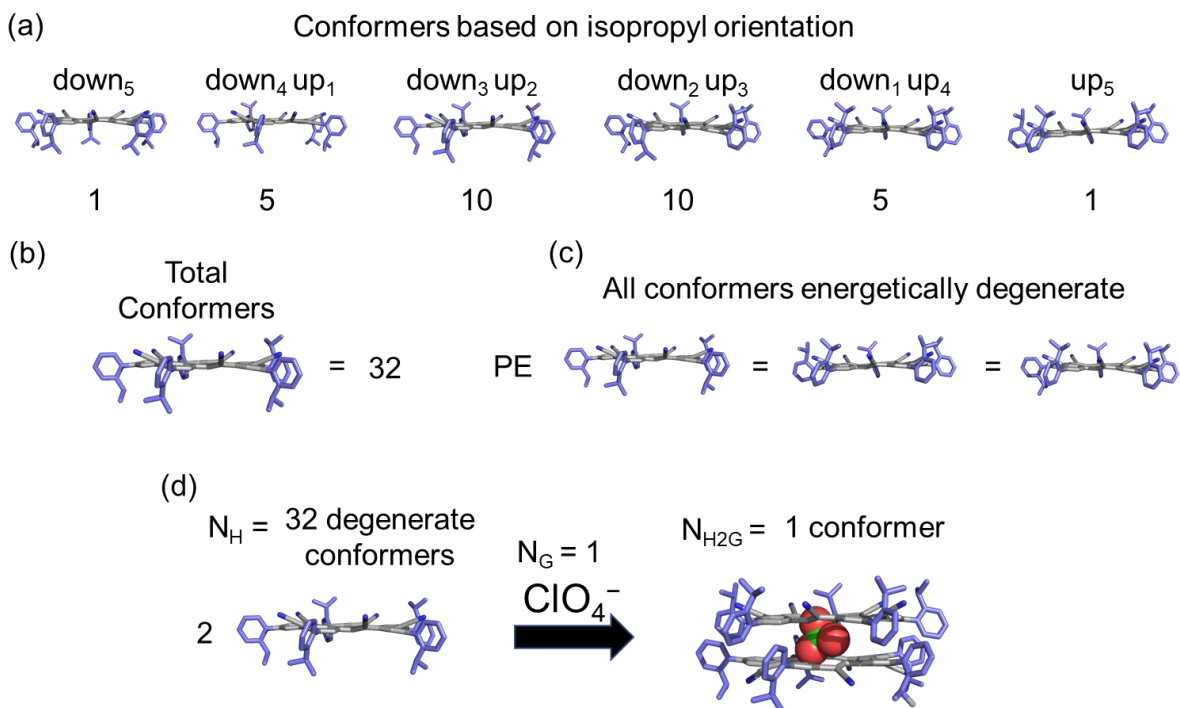


**Figure S10.** (a) Calculating the number of conformers in a free cyanodimer molecule by isopropyl orientation results in (b) 32 total lowest-energy conformers that (c) are assumed to be energetically degenerate. (d) When two macrocycles dimerize around an anion, all conformational freedom in each macrocycle is lost and one conformer remains in the 2:1 complex.

When two cyanodimer macrocycles dimerize around an anion, the rotational freedom of the isopropyl units on both macrocycles is lost and only one conformation remains accessible in the complex. Using our above assumptions, we can make a crude estimate of the configurational entropy loss cyanodimer incurs upon dimerization using the following formula:

$$\Delta S_{\text{config}}^{\circ} = -RT \ln (N_{HG} / N_H^2 N_G) \quad \text{Eq S3}$$

Where  $N_H$  is the number of degenerate conformations in the host (32),  $N_{HG}$  is the number of degenerate conformations in the host-guest complex (one), and  $N_G$  is degenerate conformations in the guest (one). This simple calculation gives a loss configurational entropy of  $\sim 57 \text{ J K}^{-1} \text{ mol}^{-1}$  or loss in stability of  $\sim 17 \text{ kJ mol}^{-1}$  at room temperature in the 2:1 cyanodimer:anion complex upon dimerization.

## S10. $^1\text{H}$ -NMR Titrations of Cyanostar and Cyanodimer with Perchlorate in $\text{CD}_2\text{Cl}_2$

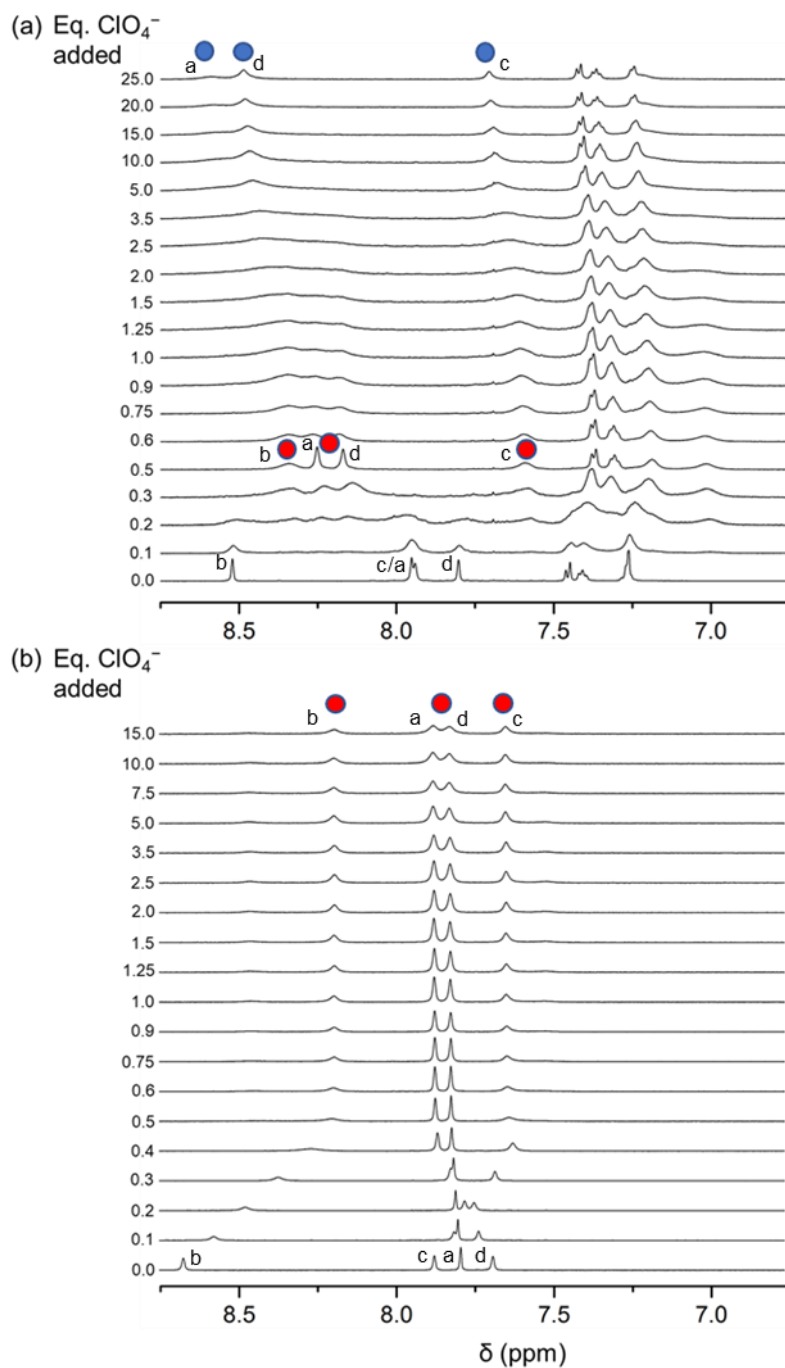


**Figure S11** (a)  $\text{ClO}_4^-$  titration with cyanodimer demonstrating the formation of a 2:1 complex followed by a 1:1 complex, with stoichiometries defined by analogy to cyanostar (2:1) and cyanosolo (1:1) (1 mM,  $\text{CD}_2\text{Cl}_2$ , 298 K, 600 MHz). (b)  $\text{ClO}_4^-$  titration with cyanostar demonstrating the formation of only a 2:1 complex (1 mM,  $\text{CD}_2\text{Cl}_2$ , 298 K, 600 MHz). In both spectra, the 2:1 complex is labelled with red dots and the 1:1 complex is labelled with blue dots

### S11. Variable Temperature $^1\text{H-NMR}$ Titrations of Cyanostar and Cyanodimer with Perchlorate in $\text{C}_2\text{D}_2\text{Cl}_4$

To test for the role of entropy in the loss of cooperativity, we heated the sample to confirm that we could destabilize the 2:1 complex of cyanodimer to a greater extent than cyanostar. The distribution of complexes with one equivalent of added  $\text{TBAClO}_4$  was examined by  $^1\text{H}$  NMR spectroscopy (280  $\mu\text{M}$ , Figure S10-S11). Four temperatures from 298 to 353 K were examined predicting use of tetrachloroethane ( $\text{CDCl}_2\text{CDCl}_2$ ). We used tetrachloroethane as a higher boiling point halogenated solvent of similar polarity to dichloromethane to reach higher temperatures. Cyanostar remained stable as a 2:1 complex across all temperatures and simply showed a cross over from slow to fast exchange beyond 333 K. Cyanodimer, however, transitioned from a mixture of the 1:1 and 2:1 complexes to a fast-exchanging mixture of free cyanodimer and the 1:1 complex at 333 K. The loss in 2:1 complex for cyanodimer verifies a stronger entropic penalty than the parent cyanostar and supports our hypothesis that cyanodimer's cooperativity is impeded by an entropic cost to dimerization caused by restricting rotations of the 10 biphenyl units.

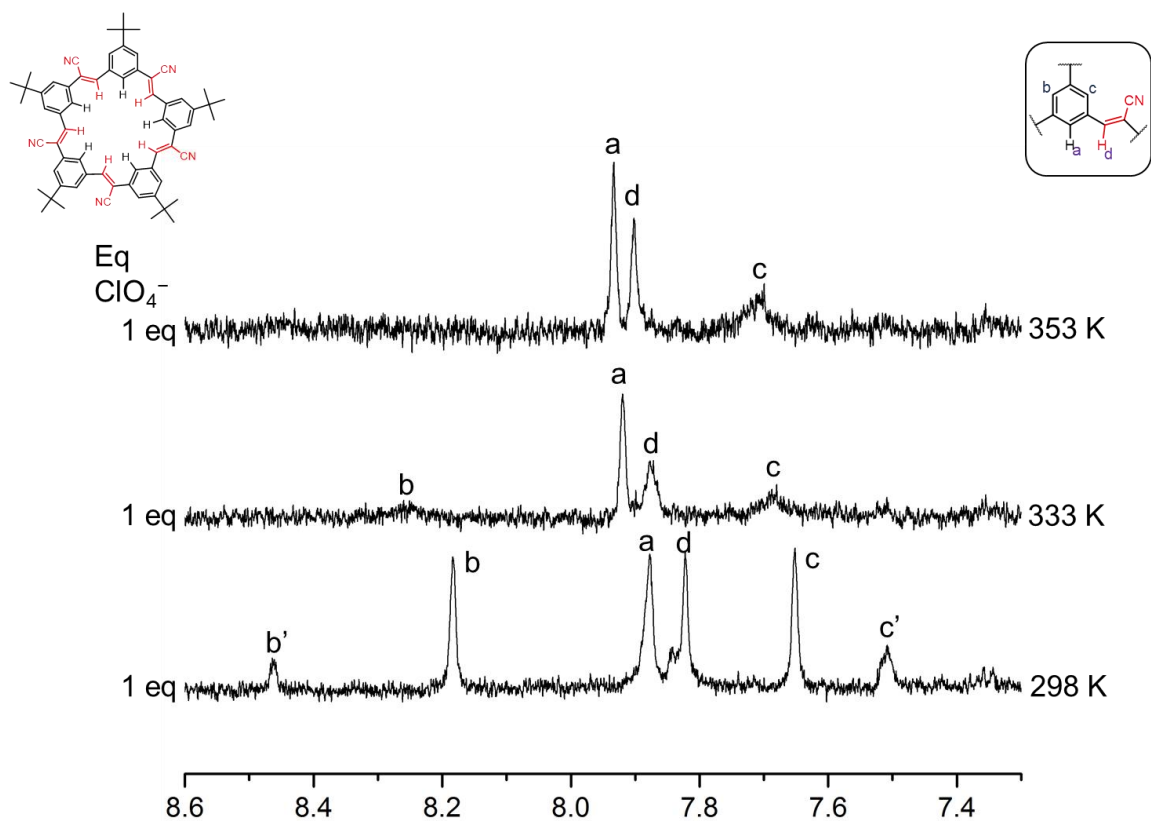


**Figure S12.** Variable temperature  $^1\text{H-NMR}$  spectra of cyanostar with 1 equivalent  $\text{TBAClO}_4$  (280  $\mu\text{M}$ ,  $\text{C}_2\text{D}_2\text{Cl}_4$ , 500 MHz)

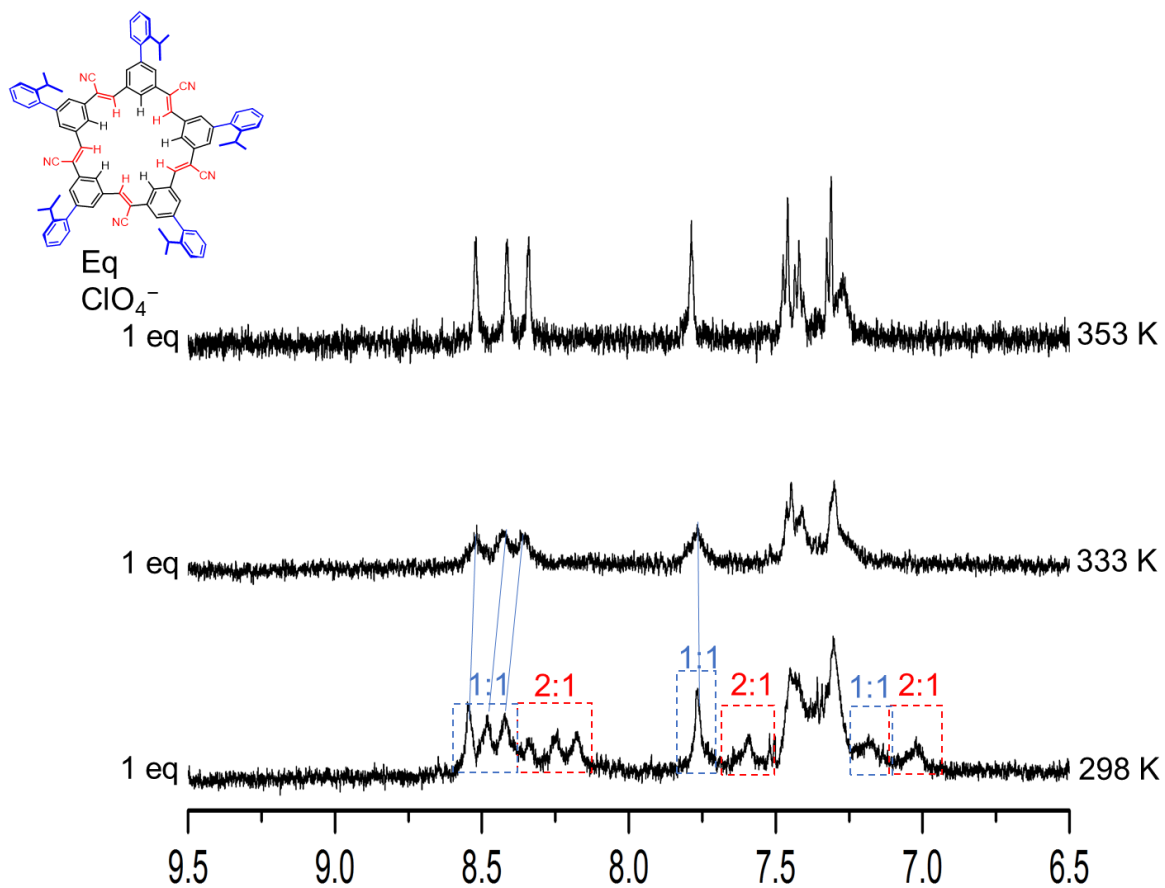


**Figure S13.** Variable temperature <sup>1</sup>H-NMR spectra of cyanostar with 1 equivalent TBAClO<sub>4</sub> (280 μM, C<sub>2</sub>D<sub>2</sub>Cl<sub>4</sub>, 500 MHz)

## S12. Variable Temperature UV-Visible Titrations of Cyanostar and Cyanodimer with Perchlorate in $C_2H_4Cl_2$

Titration data were analyzed globally by equilibrium restricted factor analysis using Sivvu.<sup>S13</sup>

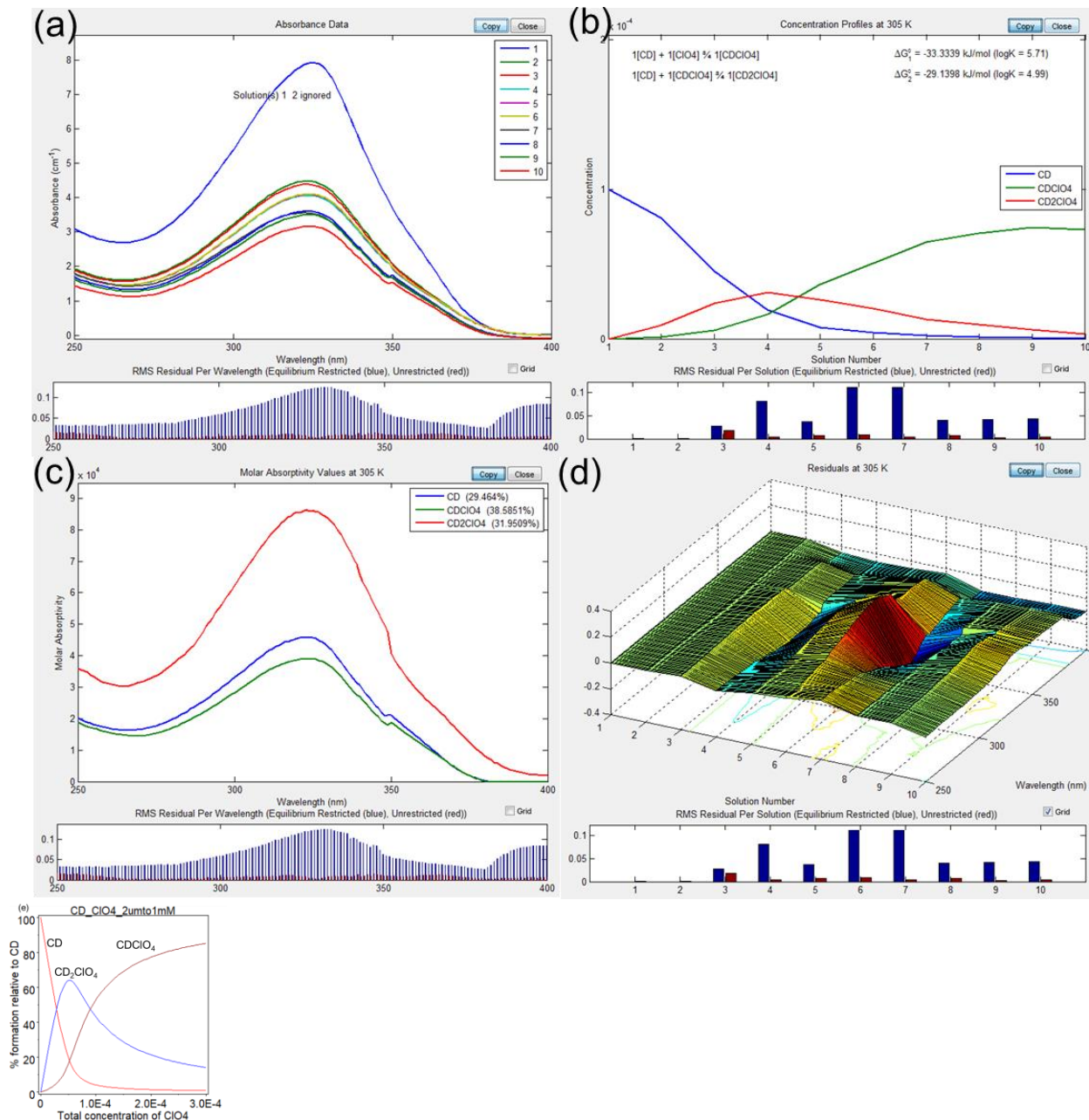


**Figure S14.** UV-Vis titration of cyanodimer (100  $\mu$ M) in  $C_2H_4Cl_2$  at 305 K. (a) Raw absorbance data. (b) Concentration profile generated from free energies. (c) Sivvu-generated absorptivity plots of cyanodimer complexes. (d) Residuals obtained from the full data set across all equivalents of  $ClO_4^-$  and all wavelengths. (e) Hyss-generated speciation curve for cyanodimer (100  $\mu$ M) and  $ClO_4^-$  using experimentally determined free energies.

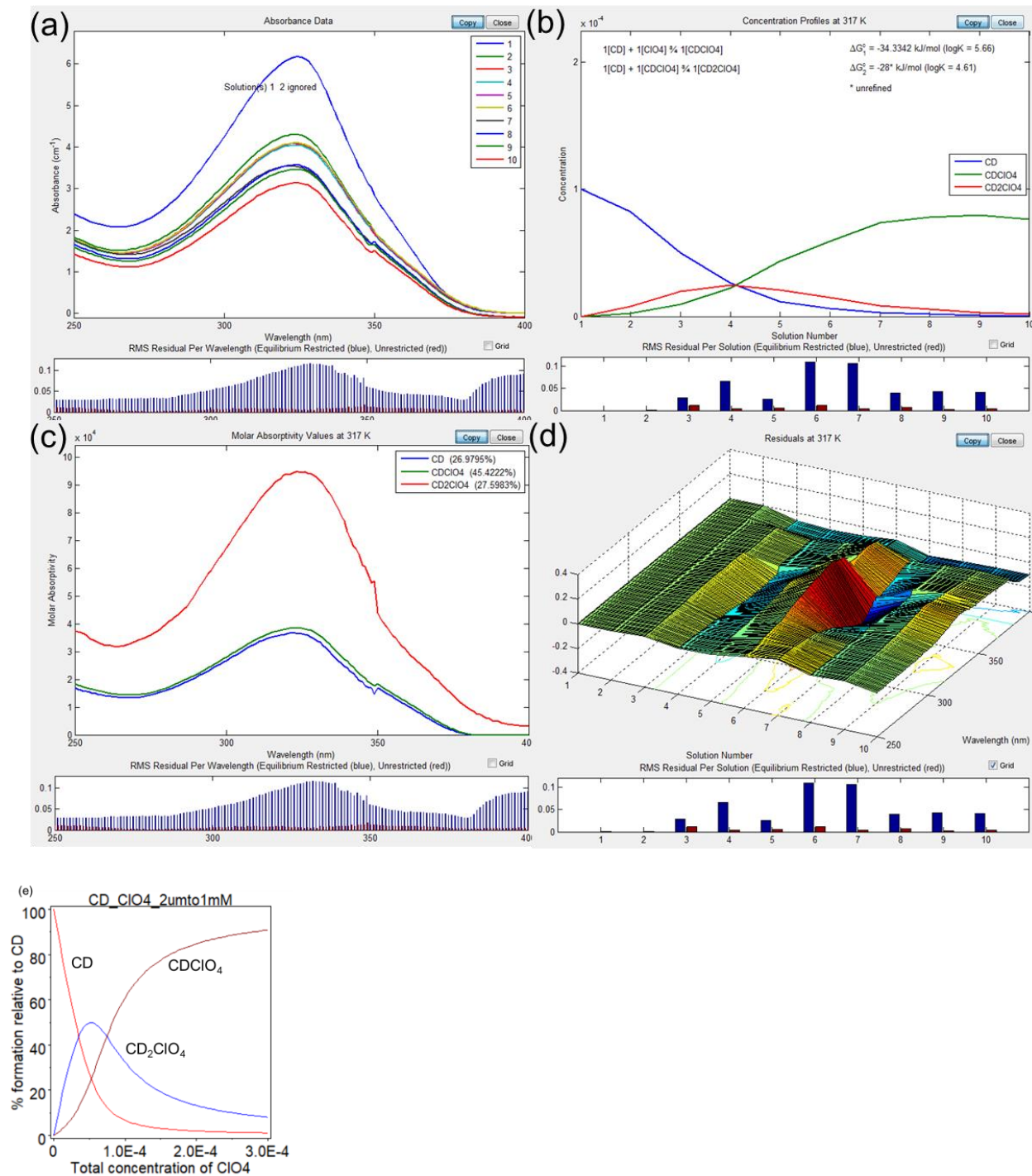


**Figure S15.** UV-Vis titration of cyanodimer (100  $\mu\text{M}$ ) in  $\text{C}_2\text{H}_4\text{Cl}_2$  at 317 K. (a) Raw absorbance data. (b) Concentration profile generated from free energies. (c) Sivvu-generated absorptivity plots of cyanodimer complexes. (d) Residuals obtained from the full data set across all equivalents of  $\text{ClO}_4^-$  and all wavelengths. (e) Hyss-generated speciation curve for cyanodimer (100  $\mu\text{M}$ ) and  $\text{ClO}_4^-$  using experimentally determined free energies.

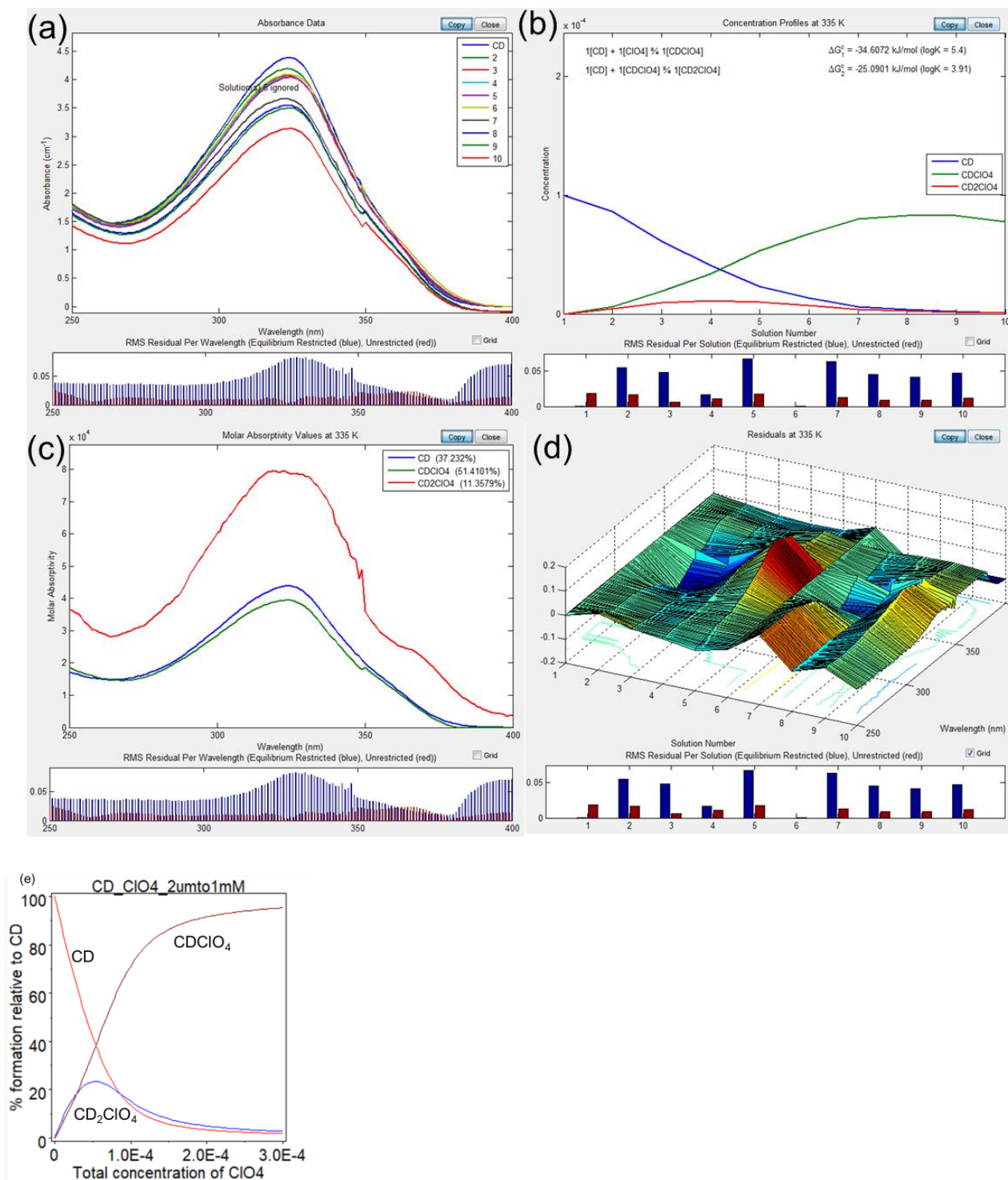


**Figure S16.** UV-Vis titration of cyanodimer (100  $\mu\text{M}$ ) in  $\text{C}_2\text{H}_4\text{Cl}_2$  at 335 K. (a) Raw absorbance data. (b) Concentration profile generated from free energies. (c) Sivvu-generated absorptivity plots of cyanodimer complexes. (d) Residuals obtained from the full data set across all equivalents of  $\text{ClO}_4^-$  and all wavelengths. (e) Hyss-generated speciation curve for cyanodimer (100  $\mu\text{M}$ ) and  $\text{ClO}_4^-$  using experimentally determined free energies.

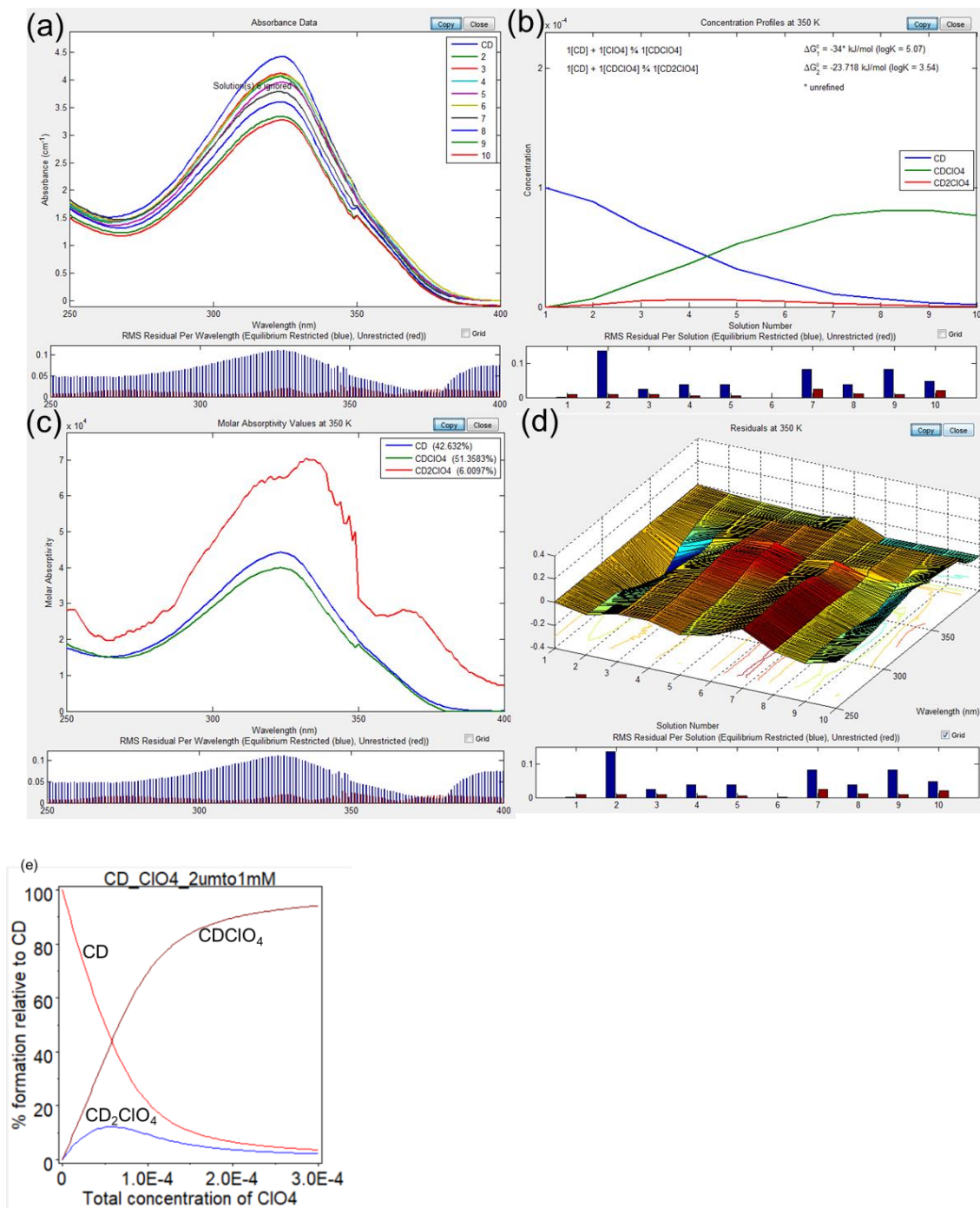


**Figure S17.** UV-Vis titration of cyanodimer (100  $\mu\text{M}$ ) in  $\text{C}_2\text{H}_4\text{Cl}_2$  at 350 K. (a) Raw absorbance data. (b) Concentration profile generated from free energies. (c) Sivvu-generated absorptivity plots of cyanodimer complexes. (d) Residuals obtained from the full data set across all equivalents of  $\text{ClO}_4^-$  and all wavelengths. (e) Hyss-generated speciation curve for cyanodimer (100  $\mu\text{M}$ ) and  $\text{ClO}_4^-$  using experimentally determined free energies.  $K_2$  generated by fixing  $K_1$  based on  $K_1$  generated when the  $K_2$  equilibrium is excluded (Figure S16 cont.)

### 350 K 1 equilibrium

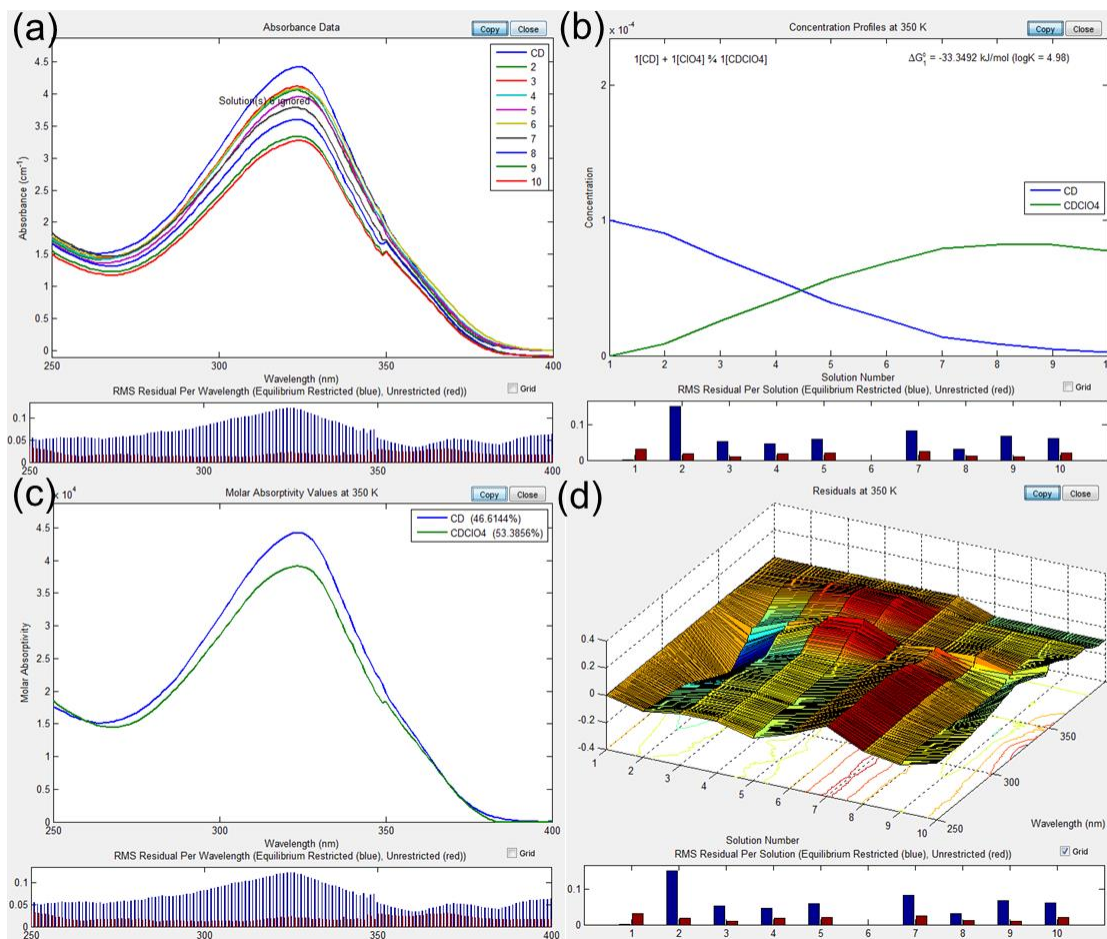


**Figure S17 (cont.).** UV-Vis titration of cyanodimer (100  $\mu\text{M}$ ) in  $\text{C}_2\text{H}_4\text{Cl}_2$  at 350 K with the 2:1 equilibrium omitted. (a) Raw absorbance data. (b) Concentration profile generated from free energies. (c) Sivvu-generated absorptivity plots of cyanodimer complexes. (d) Residuals obtained from the full data set across all equivalents of  $\text{ClO}_4^-$  and all wavelengths.

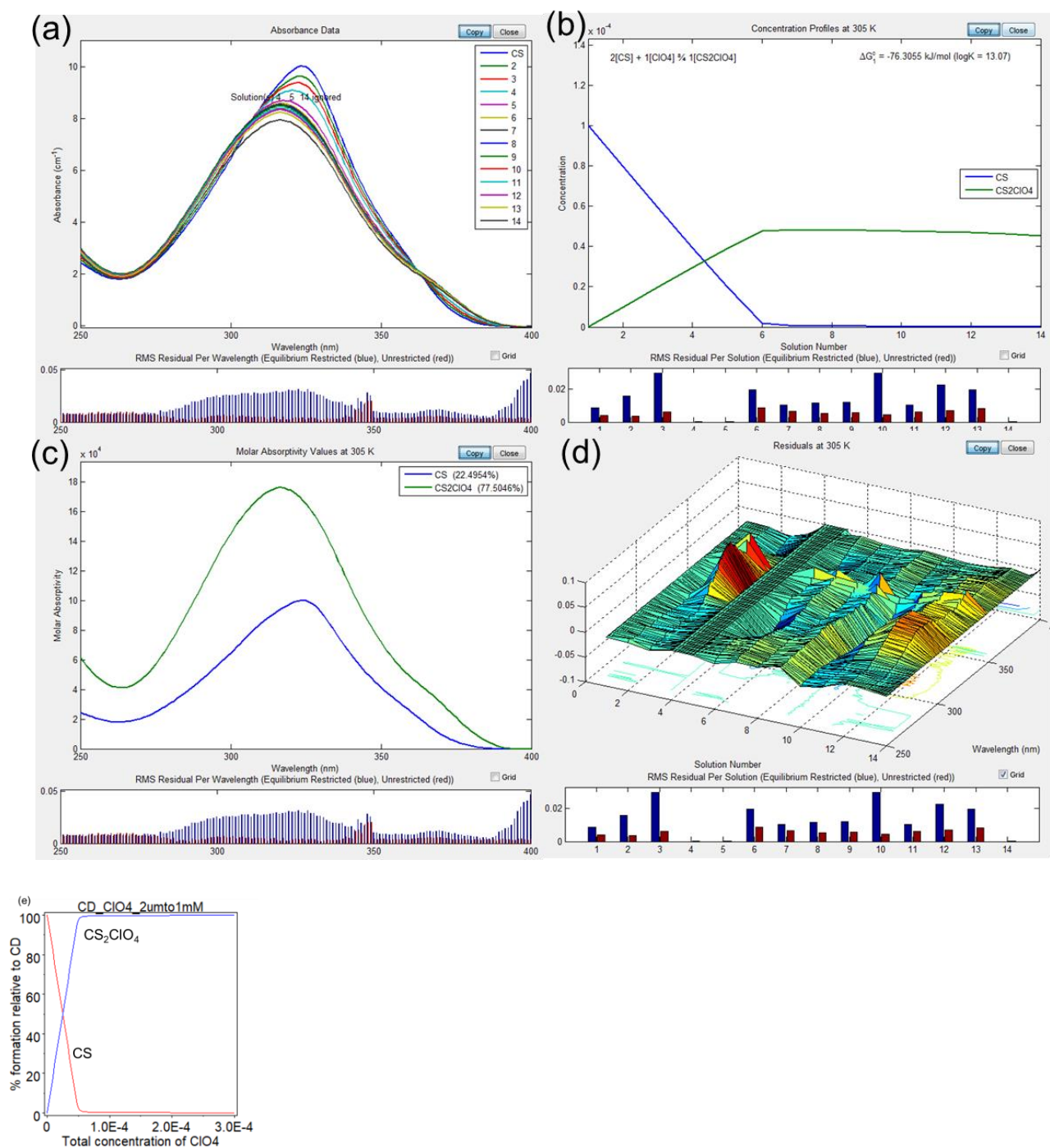


**Figure S18.** UV-Vis titration of cyanostar (100  $\mu\text{M}$ ) in  $\text{C}_2\text{H}_4\text{Cl}_2$  at 305 K. (a) Raw absorbance data. (b) Concentration profile generated from free energies. (c) Sivvu-generated absorptivity plots of cyanostar complexes. (d) Residuals obtained from the full data set across all equivalents of  $\text{ClO}_4^-$  and all wavelengths. (e) Hyss-generated speciation curve for cyanostar (100  $\mu\text{M}$ ) and  $\text{ClO}_4^-$  using experimentally determined free energies.

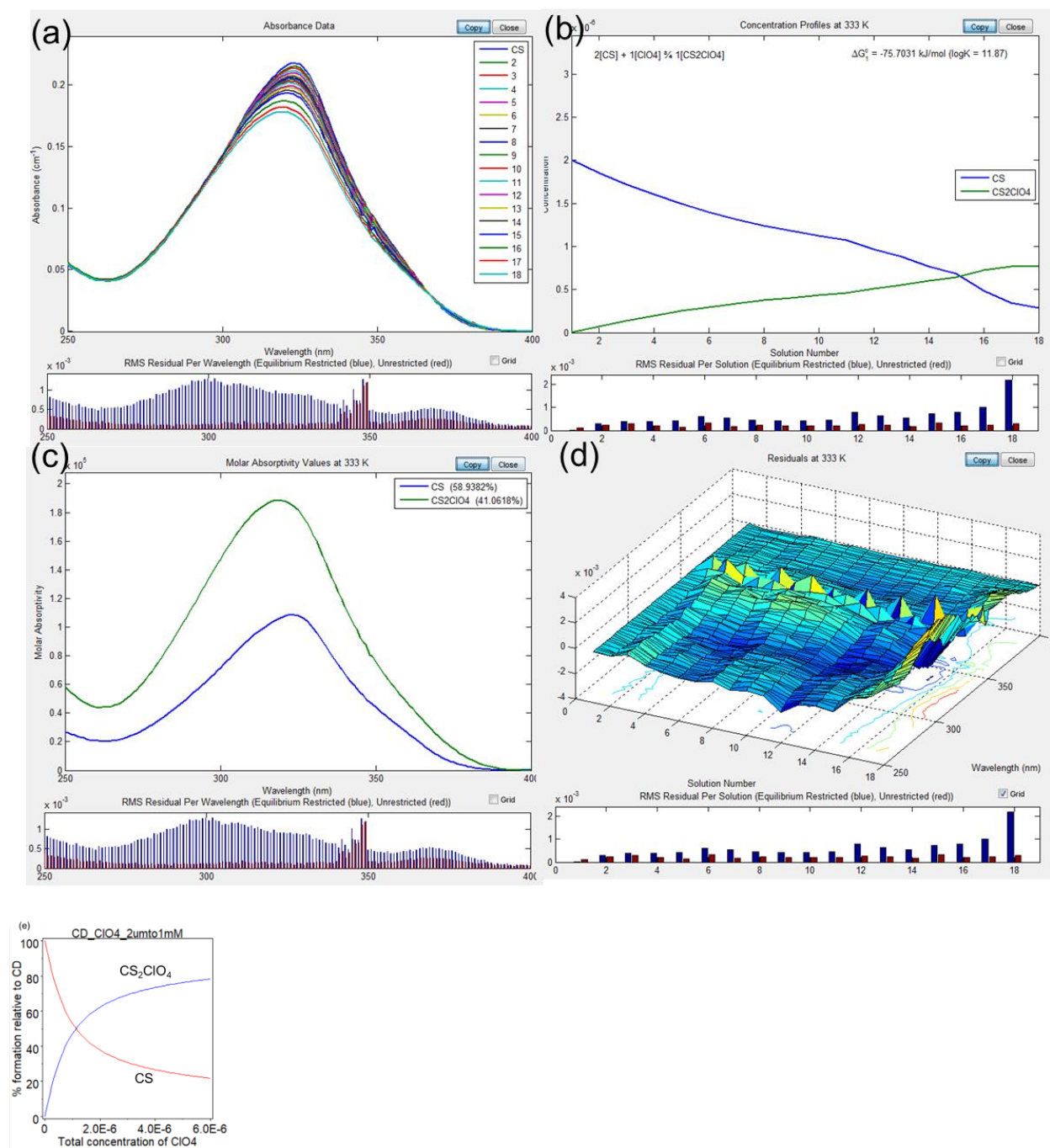


**Figure S19.** UV-Vis titration of cyanostar (2  $\mu\text{M}$ ) in  $\text{C}_2\text{H}_4\text{Cl}_2$  at 317 K. (a) Raw absorbance data. (b) Concentration profile generated from free energies. (c) Sivvu-generated absorptivity plots of cyanostar complexes. (d) Residuals obtained from the full data set across all equivalents of  $\text{ClO}_4^-$  and all wavelengths. (e) Hyss-generated speciation curve for cyanostar (2  $\mu\text{M}$ ) and  $\text{ClO}_4^-$  using experimentally determined free energies.

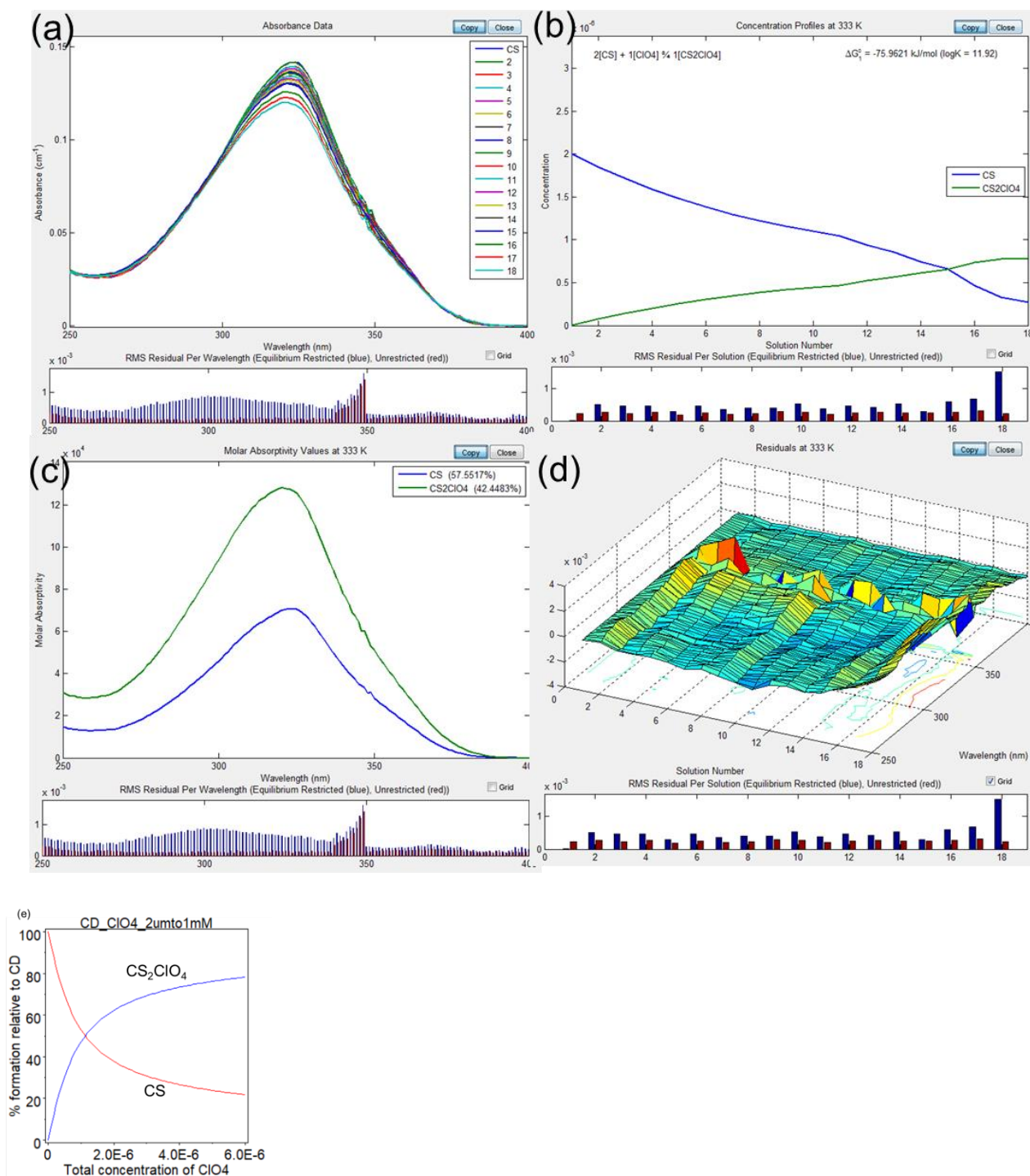


**Figure S20.** UV-Vis titration of cyanostar (2  $\mu\text{M}$ ) in  $\text{C}_2\text{H}_4\text{Cl}_2$  at 333 K. (a) Raw absorbance data. (b) Concentration profile generated from free energies. (c) Sivvu-generated absorptivity plots of cyanostar complexes. (d) Residuals obtained from the full data set across all equivalents of  $\text{ClO}_4^-$  and all wavelengths. (e) Hyss-generated speciation curve for cyanostar (2  $\mu\text{M}$ ) and  $\text{ClO}_4^-$  using experimentally determined free energies.

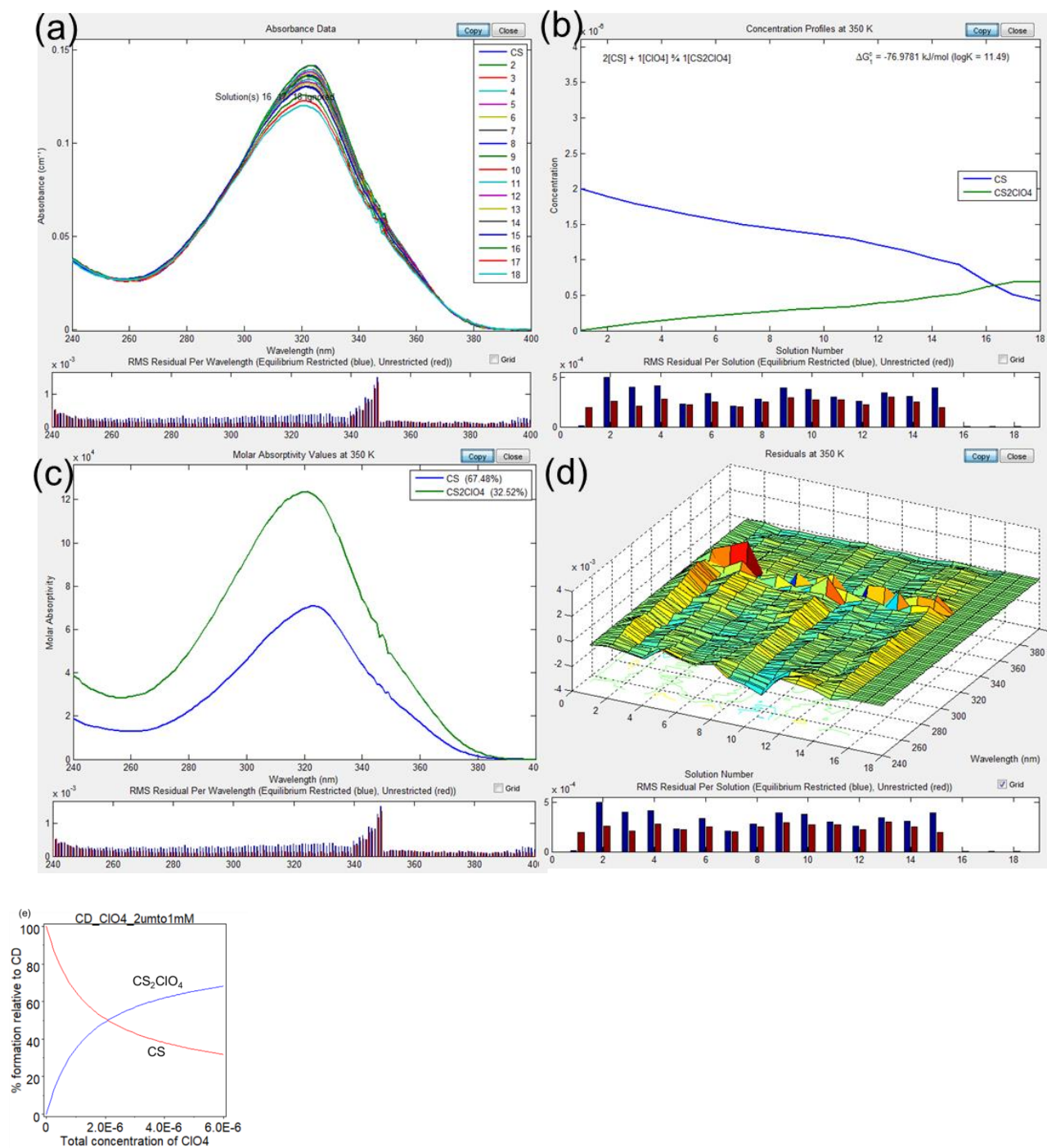


**Figure S21.** UV-Vis titration of cyanostar (2  $\mu\text{M}$ ) in  $\text{C}_2\text{H}_4\text{Cl}_2$  at 350 K. (a) Raw absorbance data. (b) Concentration profile generated from free energies. (c) Sivvu-generated absorptivity plots of cyanostar complexes. (d) Residuals obtained from the full data set across all equivalents of  $\text{ClO}_4^-$  and all wavelengths. (e) Hyss-generated speciation curve for cyanostar (2  $\mu\text{M}$ ) and  $\text{ClO}_4^-$  using experimentally determined free energies.

**Table 1. Experimental thermodynamic data for cyanodimer 2:1 complexation with perchlorate**

$T$ (K)	$\Delta G_{2:1}$ (kJ / mol)	$-T \Delta S_{2:1}$ (kJ / mol)
303	$-63 \pm 4$	35
317	$-62 \pm 2$	36
333	$-59 \pm 4$	38
350	$-58 \pm 2$	40

$\Delta H_{2:1}$  (kJ / mol):  $-98 \pm 6$

$\Delta S_{2:1}$  (J mol<sup>-1</sup> K<sup>-1</sup>):  $-115 \pm 18$

$\Delta \Delta S_{2:1}$  CS:CD (J mol<sup>-1</sup> K<sup>-1</sup>):  $103 \pm 34$

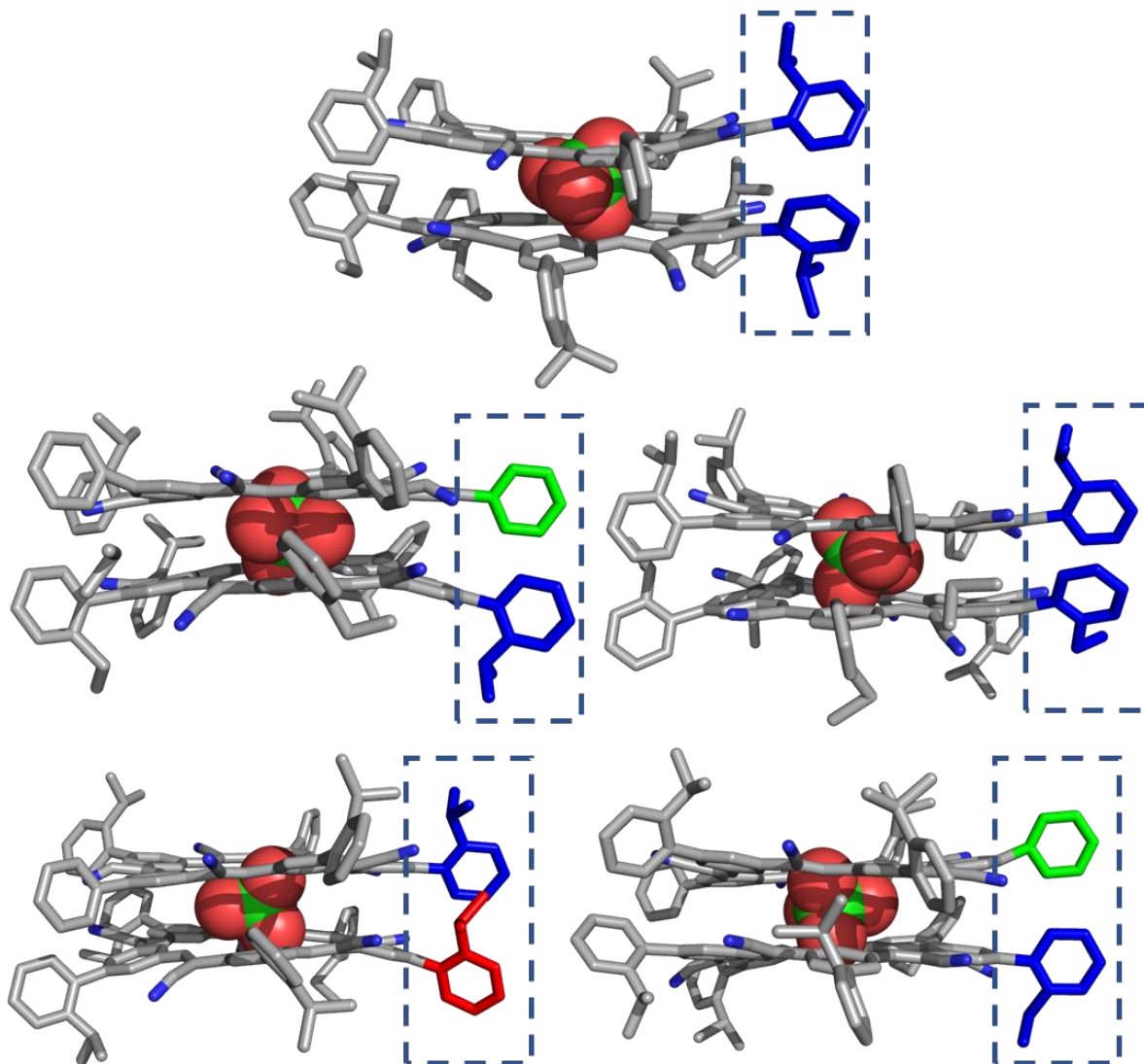
**Table 2. Experimental thermodynamic data for cyanostar 2:1 complexation with perchlorate**

$T$ (K)	$\Delta G_{2:1}$ (kJ / mol)	$-T \Delta S_{2:1}$ (kJ / mol)
303	$-76.3 \pm 1$	-4
317	$-75.7 \pm 0.1$	-4
333	$-75.9 \pm 0.2$	-4
350	$-77.0 \pm 0.3$	-4

$\Delta H_{2:1}$  (kJ / mol):  $-72.3 \pm 5.1$

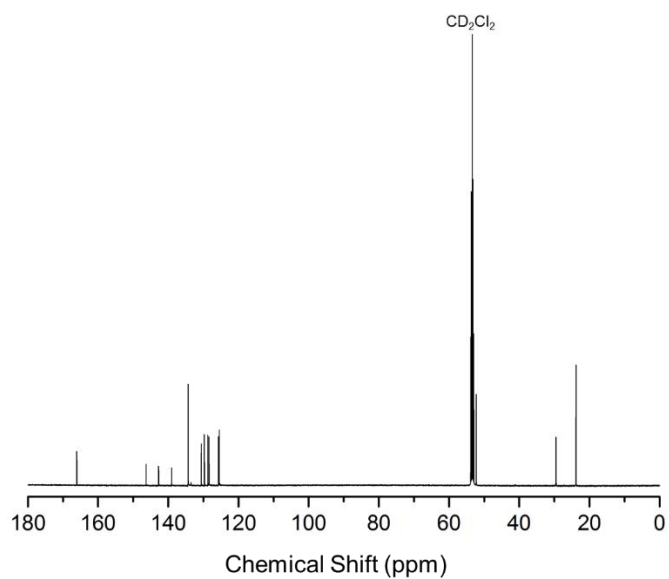
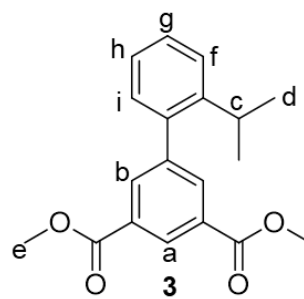
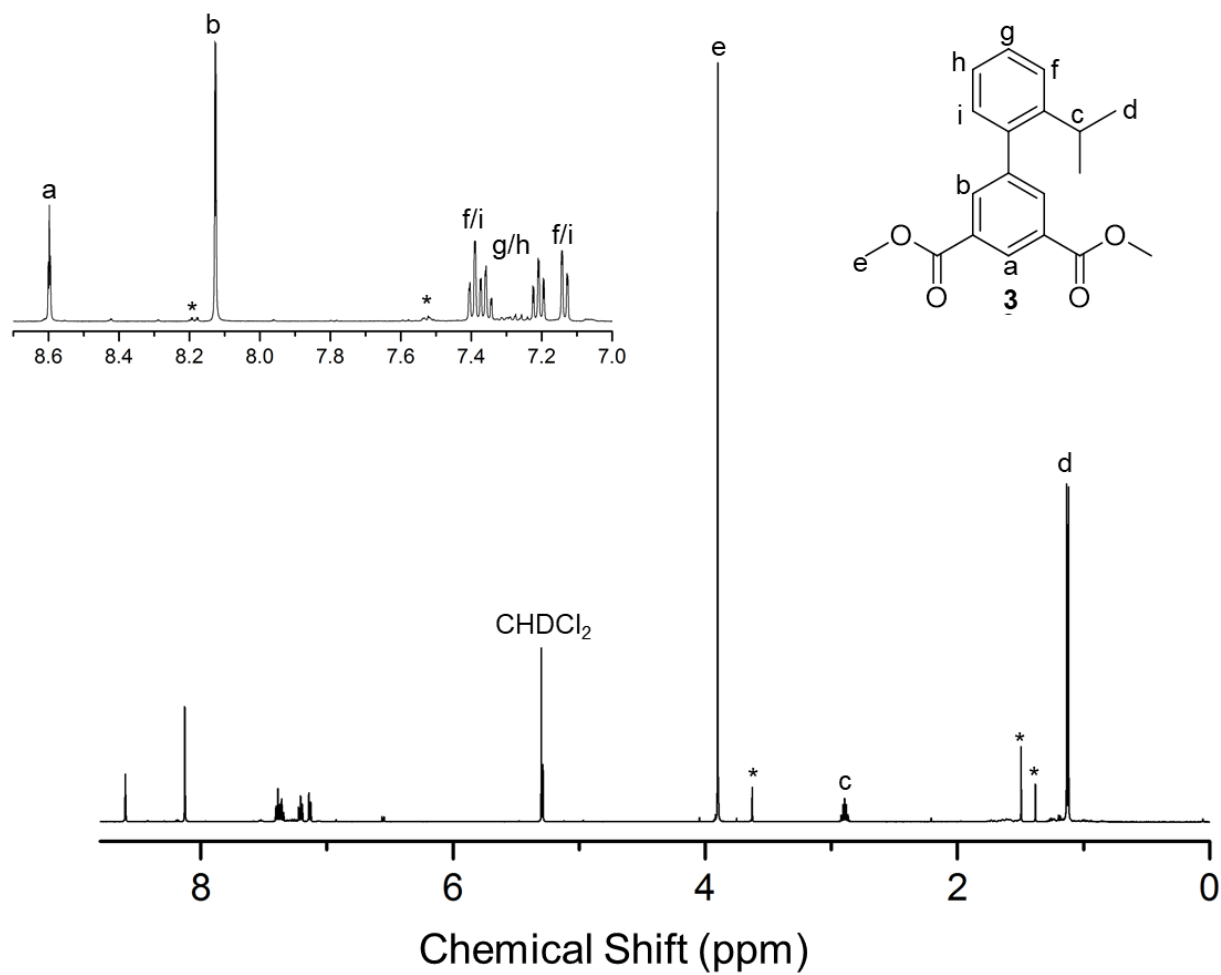
$\Delta S_{2:1}$  (J mol<sup>-1</sup> K<sup>-1</sup>):  $12 \pm 16$

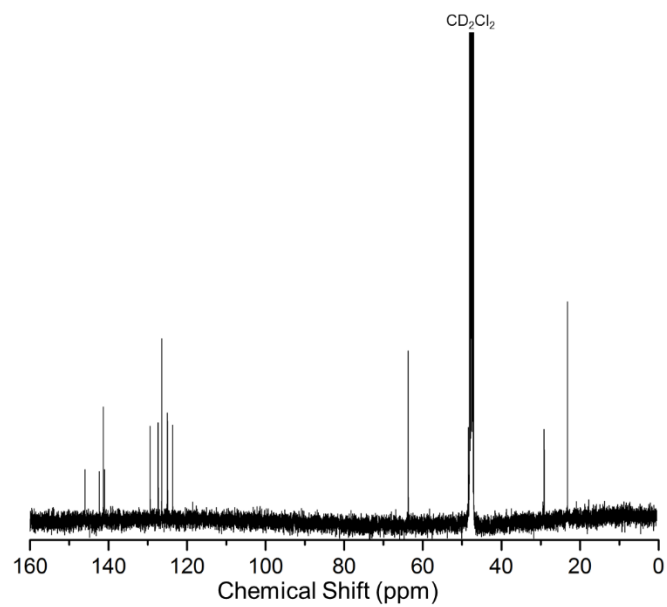
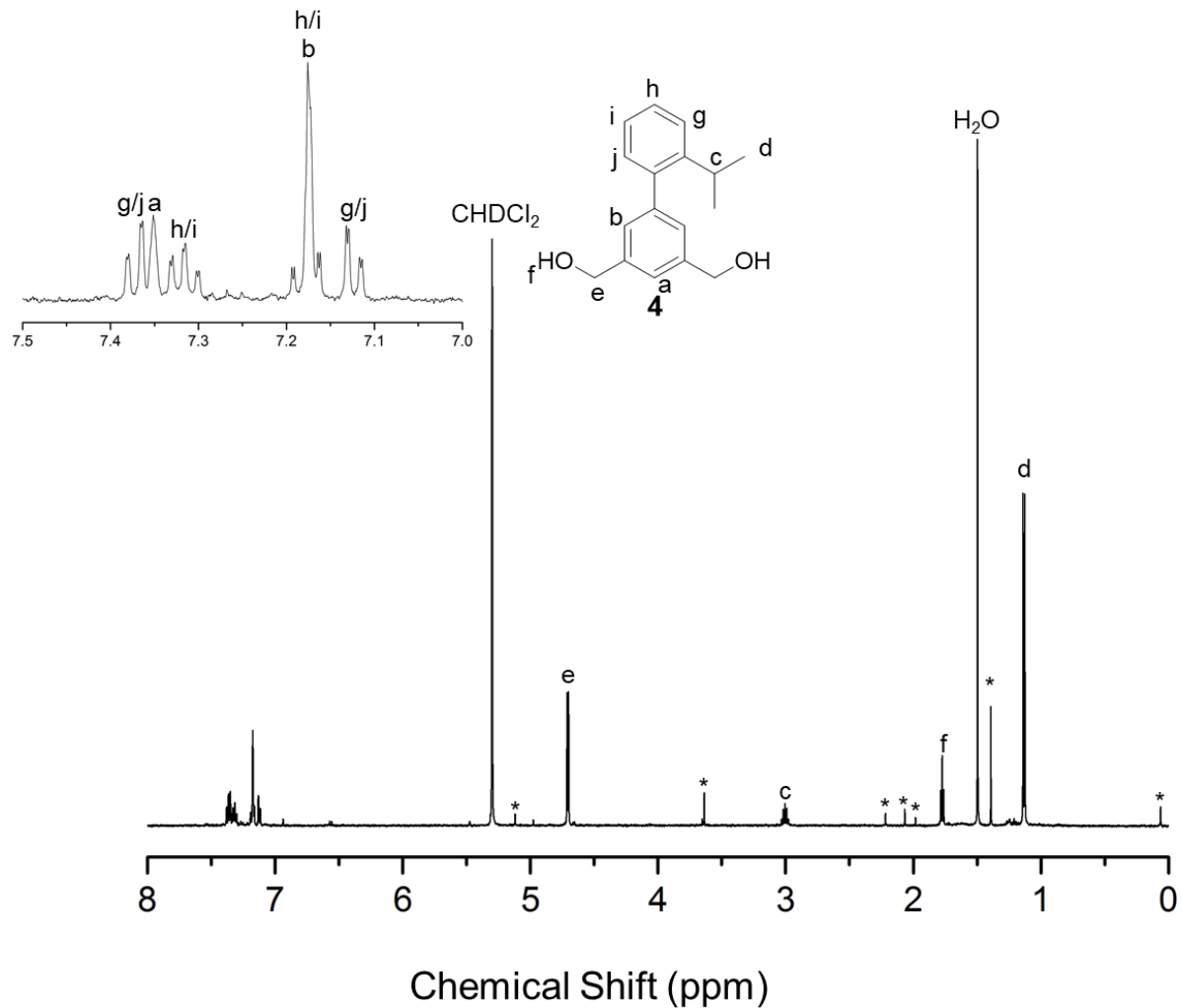
### S13. Configurational Information for the Preliminary Crystal Structure

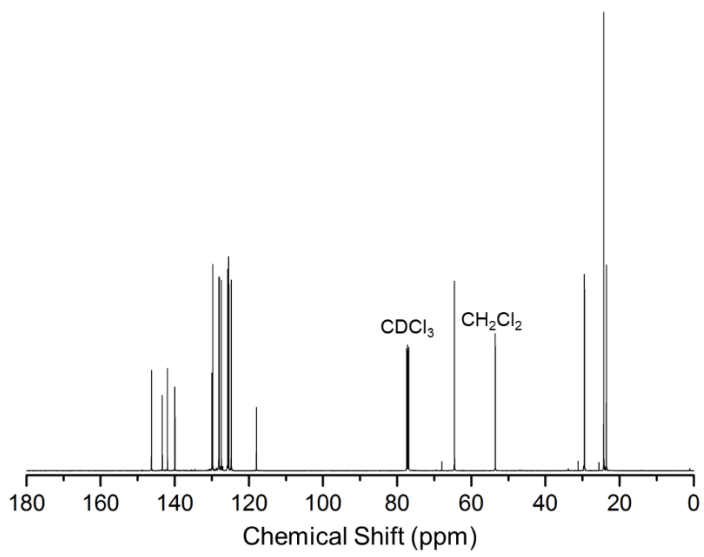
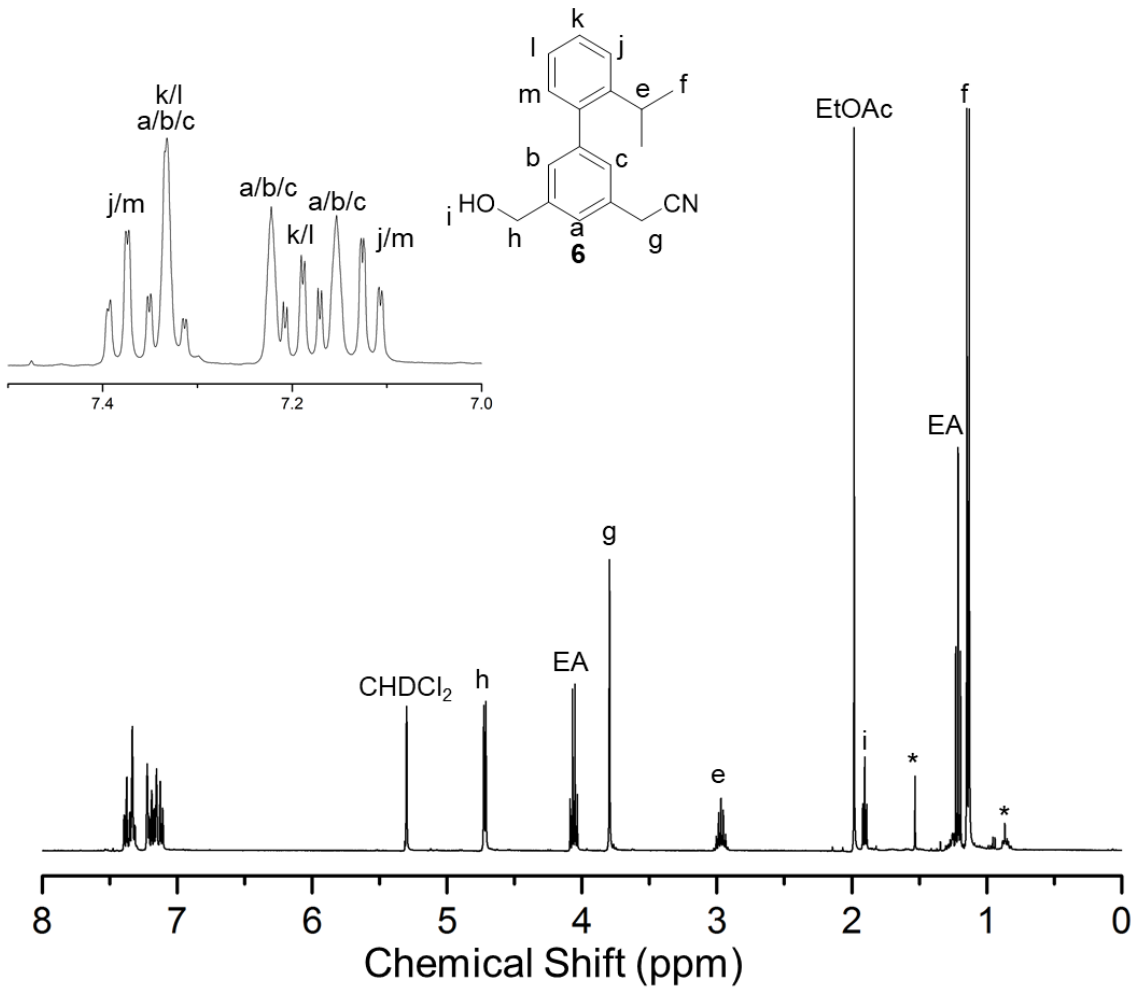


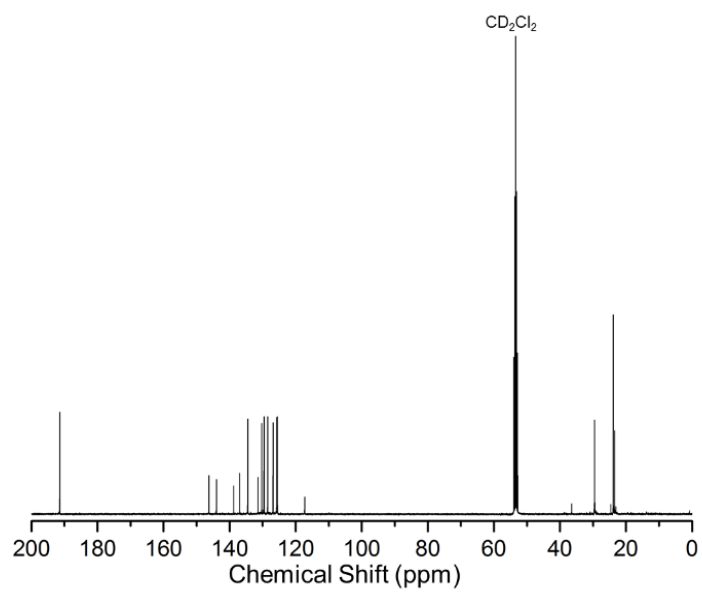
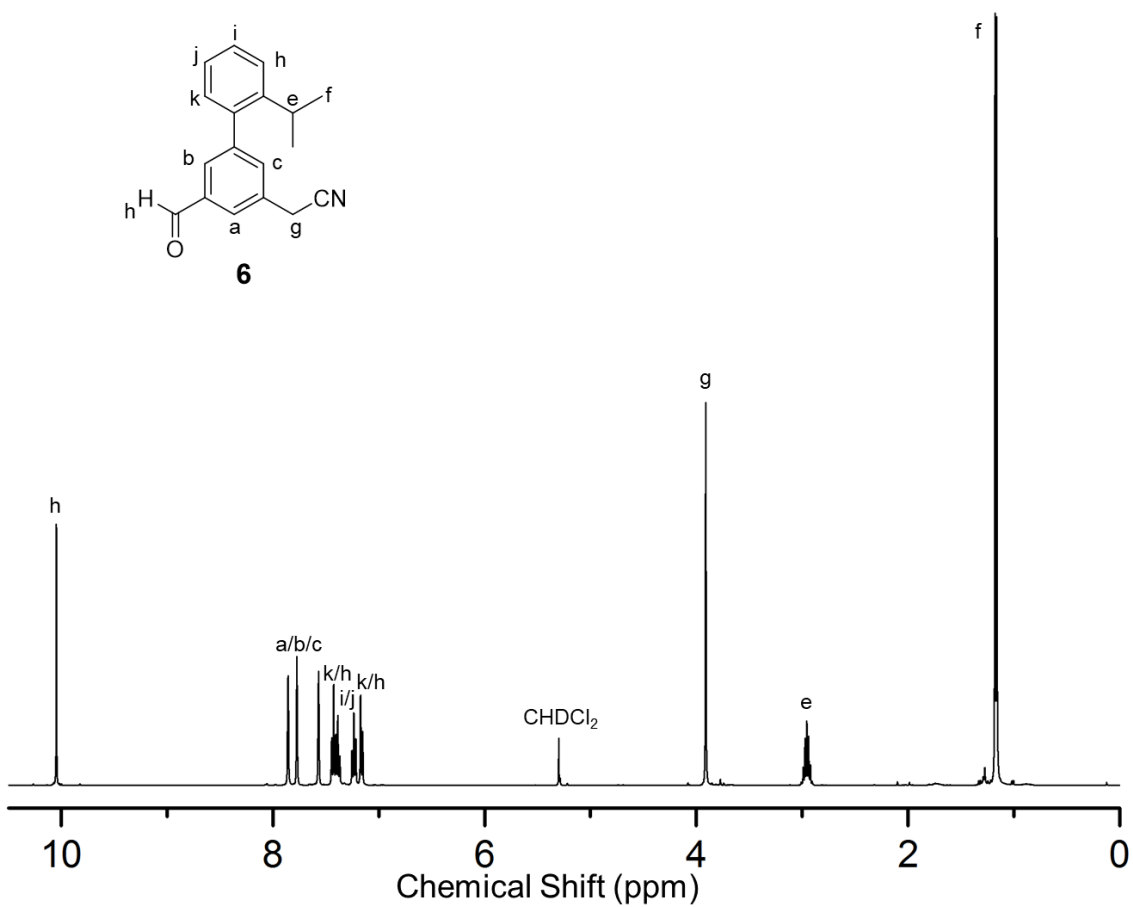
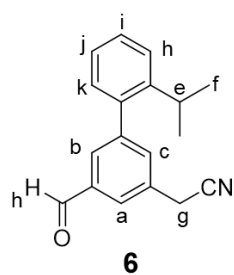
**Figure S22.** Five views of the preliminary crystal structure showing the orientations and disorder in the substituents. Red indicates that the isopropyl group is facing inwards towards the macrocycle-macrocycle seam, blue indicates the isopropyl group is facing outward, away from the seam, and green indicates that the data is not well-resolved enough to assign an orientation.

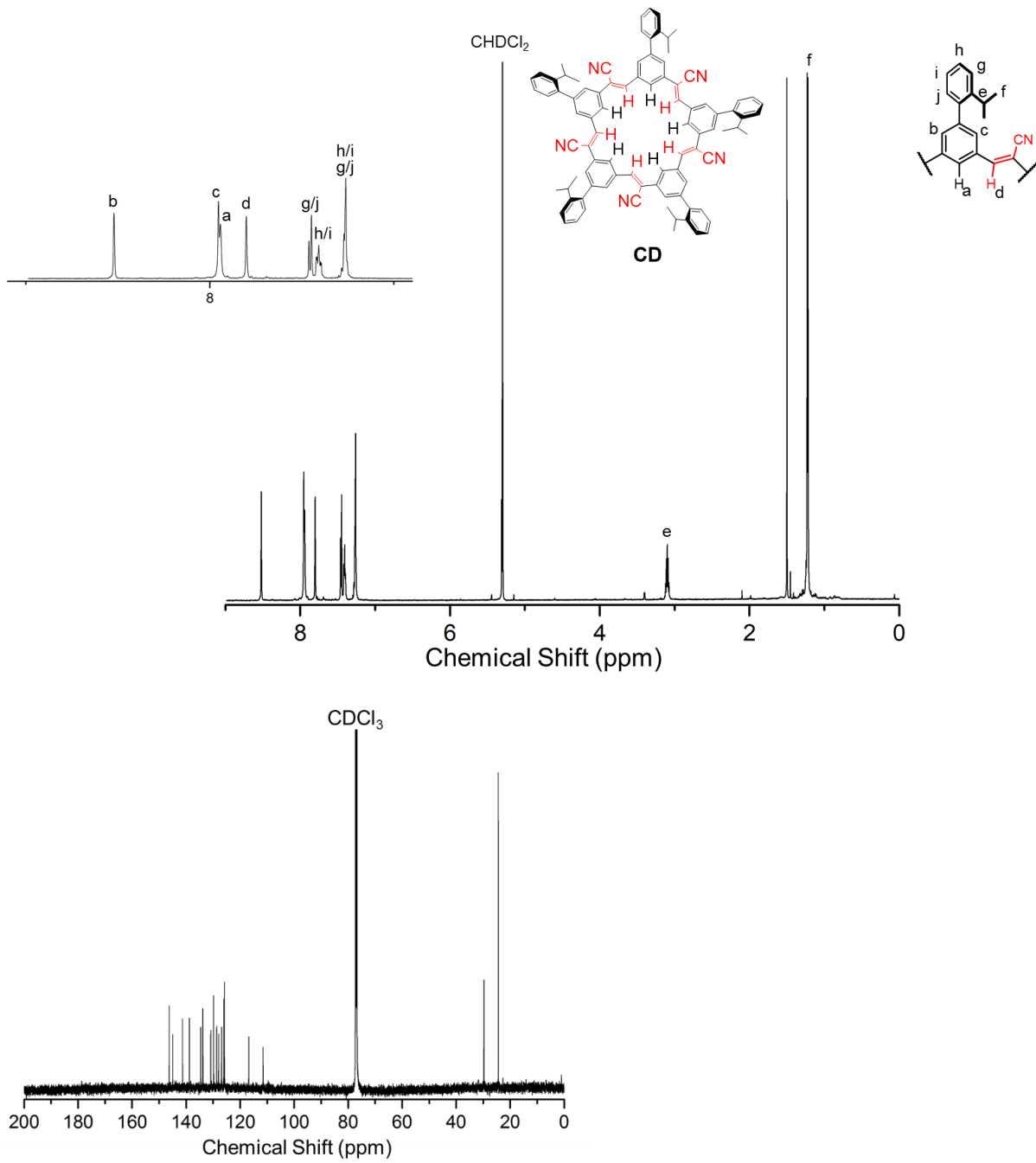
**S14.  $^1\text{H}$  and  $^{13}\text{C}$  NMR Spectra** (\*) denotes impurities











## References

- S1. Park, J.; Wang, Z. U.; Sun, L.-B.; Chen, Y.-P.; Zhou, H.-C. *J. Am. Chem. Soc.* **2012**, *134*, 20110-20116.
- S2. Lee, S.; Chen, C.-H.; Flood, A. H. *Nat. Chem.* **2013**, *5*, 704-710
- S3. Hirsch, B. E.; Lee, S.; Qiao, B.; Chen, C.-H.; McDonald, K. P.; Tait, S. L.; Flood, A. H.; *Chem. Commun.* **2014**, *69*, 9827-9830
- S4. Qiao, B.; Anderson, J. R.; Pink, M.; Flood, A. H. *Chem. Commun.* **2016**, *52*, 8683-8686.
- S5. Fatila, E. M.; Twum, E. B.; Sengupta, A.; Pink, M.; Karty, J. A.; Raghavachari, K.; Flood, A. H., *Angew. Chem. Int. Ed.* **2016**, *55*, 14057-14062.
- S6. Benson, C. R.; Fatila, E. M.; Lee, S.; Marzo, M. G.; Pink, M.; Mills, M. B.; Preuss, K. E.; Flood, A. H. *J. Am. Chem. Soc.* **2016**, *138*, 15057-15065
- S7. Qiao, B.; Liu, Y.; Lee, S.; Pink, M.; Flood, A. H.; *Chem. Commun.* **2016**, *52*, 13675-13678.
- S8. Qiao, B.; Hirsch, B. E.; Lee, S.; Pink, M.; Chen, C.-H.; Laursen, B. W.; Flood, A. H. *J. Am. Chem. Soc.* **2017**, *139*, 6226-6233.
- S9. Fatila, E. M.; Twum, E. B.; Karty, J. A.; Flood, A. H.; *Chem. Eur. J.* **2017**, *23*, 10652-10662
- S10. Zhao, W.; Qiao, B.; Chen, C.-H.; Flood, A. H. *Angew. Chem. Int. Ed.* **2017**, *56*, 13083-13087.
- S11. Fatila, E. M.; Pink, M.; Twum, E. B.; Karty, J. A.; Flood, A. H. *Chem. Sci.*, **2018**, *9*, accepted.
- S12. Mammen, M.; Shakhnovich, E. I.; Whitesides, G. M. *J. Org. Chem.* **1998**, *63*, 3168-3175.
- S13. Vander Griend, D. A., Bediako, D. K., DeVries, M. J., DeJong, N. A. & Heeringa, L. P. *Inorg. Chem.* **2008**, *47*, 656-662.